Consistent Formulations of the Interaction Integral Method for Fracture of Functionally Graded Materials

Jeong-Ho Kim[1]

Glaucio H. Paulino[2]
e-mail: paulino@uiuc.edu

Department of Civil and Environmental Engineering,
Newmark Laboratory,
The University of Illinois at Urbana-Champaign,
205 North Mathews Avenue,
Urbana, IL 61801

The interaction integral method provides a unified framework for evaluating fracture parameters (e.g., stress intensity factors and T stress) in functionally graded materials. The method is based on a conservation integral involving auxiliary fields. In fracture of nonhomogeneous materials, the use of auxiliary fields developed for homogeneous materials results in violation of one of the basic relations of mechanics, i.e., equilibrium, compatibility or constitutive, which naturally leads to three independent formulations: "nonequilibrium," "incompatibility," and "constant-constitutive-tensor." Each formulation leads to a consistent form of the interaction integral in the sense that extra terms are added to compensate for the difference in response between homogeneous and nonhomogeneous materials. The extra terms play a key role in ensuring path independence of the interaction integral. This paper presents a critical comparison of the three consistent formulations and addresses their advantages and drawbacks. Such comparison is made both from a theoretical point of view and also by means of numerical examples. The numerical implementation is based on finite elements which account for the spatial gradation of material properties at the element level (graded elements).
[DOI: 10.1115/1.1876395]

1 Introduction

Solid mechanics problems consist of the following three relations:

- *equilibrium*
- *compatibility*
- *constitutive*

To determine fracture parameters, e.g., stress intensity factors (SIFs) and T stress, by means of the interaction integral (M integral[3]) method, *auxiliary fields* such as displacements ($\boldsymbol{u}^{\text{aux}}$), strains ($\boldsymbol{\varepsilon}^{\text{aux}}$), and stresses ($\boldsymbol{\sigma}^{\text{aux}}$) are needed. In fracture of functionally graded materials (FGMs), the use of the auxiliary fields developed for homogeneous materials results in violation of one of the three relations earlier, which leads to three independent formulations (see Fig. 1): nonequilibrium, incompatibility, and constant-constitutive-tensor formulations. Each formulation leads to a different final form of the resulting M integral, and for *consistency*, extra terms are added to compensate for the difference in response between homogeneous and nonhomogeneous materials. Table 1 illustrates the auxiliary fields corresponding to each formulation. Notice that the nonequilibrium formulation satisfies compatibility ($\boldsymbol{\varepsilon}^{\text{aux}}=(\text{sym}\nabla)\boldsymbol{u}^{\text{aux}}$) and the constitutive relations ($\boldsymbol{\sigma}^{\text{aux}}=\boldsymbol{C}(\boldsymbol{x})\boldsymbol{\varepsilon}^{\text{aux}}$), but violates equilibrium ($\nabla\cdot\boldsymbol{\sigma}^{\text{aux}}\neq 0$ with no body forces). The incompatibility formulation satisfies equilibrium and the constitutive relations, but violates compatibility conditions ($\boldsymbol{\varepsilon}^{\text{aux}}\neq(\text{sym}\nabla)\boldsymbol{u}^{\text{aux}}$). The constant-constitutive-tensor formulation satisfies equilibrium and compatibility conditions, but violates the constitutive relations ($\boldsymbol{\sigma}^{\text{aux}}=\boldsymbol{C}_{\text{tip}}\boldsymbol{\varepsilon}^{\text{aux}}$ with $\boldsymbol{C}_{\text{tip}}\neq\boldsymbol{C}(\boldsymbol{x})$). Conservation integrals based on these three consistent formulations are the focus of this paper.

This paper is organized as follows. Section 2 comments on related work. Section 3 presents auxiliary fields for SIFs and T stress. Section 4 provides three consistent formulations using the interaction integral approach. Sections 5 and 6 establish the relationships between M and SIFs and T stress, respectively. Section 7 provides comparison and critical assessment of the three consistent formulations. Sections 8 presents some numerical aspects relevant to the formulations. Section 9 presents two examples, which test different aspects of the formulations. Finally, Sec. 10 concludes this work.

2 Related Work

The interaction integral method is an accurate and robust scheme for evaluating mixed-mode SIFs and T stress. The method is formulated on the basis of conservation laws, which lead to the establishment of a conservation integral for two admissible states of an elastic solid: *actual* and *auxiliary*. Yau et al. [5] presented the interaction integral method for evaluating SIFs in homogeneous isotropic materials. Wang et al. [6] extended the method to homogeneous orthotropic materials, and Yau [7] used the method for bimaterial interface problems.

Recently, the interaction integral method has been explored in the field of fracture of FGMs. It has been extended for evaluating SIFs [8–11] in isotropic FGMs. Dolbow and Gosz [8] employed the extended finite element method (X-FEM); Rao and Rahman [9] used the element-free Galerkin method; and Kim and Paulino [10,11] used the finite element method (FEM). In addition, the

[1]Present address: Department of Civil and Environmental Engineering, The University of Connecticut, 261 Glenbrook Road U-2037, Storrs, CT 06269.

[2]To whom correspondence should be addressed.

[3]Here, the so-called M integral should not be confused with the M integral of Knowles and Sternberg [1], Budiansky and Rice [2], and Chang and Chien [3]. Also, see the book by Kanninen and Popelar [4] for a review of conservation integrals in fracture mechanics.

Contributed by the Applied Mechanics Division of THE AMERICAN SOCIETY OF MECHANICAL ENGINEERS for publication in the ASME JOURNAL OF APPLIED MECHANICS. Manuscript received by the Applied Mechanics Division, February 24, 2003; final revision, July 27, 2004. Associate Editor: K. Ravi-Chandar. Discussion on the paper should be addressed to the Editor, Professor Robert M. McMeeking, Journal of Applied Mechanics, Department of Mechanical and Environmental Engineering, University of California—Santa Barbara, Santa Barbara, CA 93106-5070, and will be accepted until four months after final publication in the paper itself in the ASME JOURNAL OF APPLIED MECHANICS.

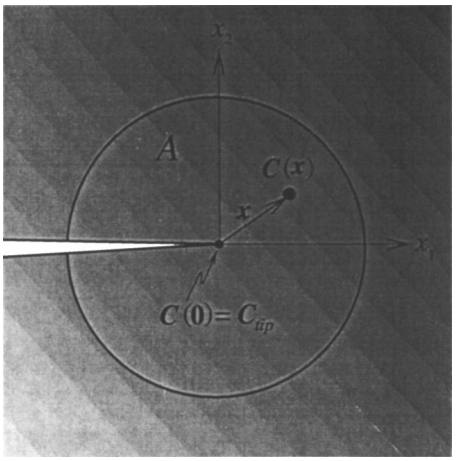

Fig. 1 Motivation for development of alternative consistent formulations. Notice that $C(x) \neq C_{tip}$ for $x \neq 0$. The area A denotes a representative region around the crack tip.

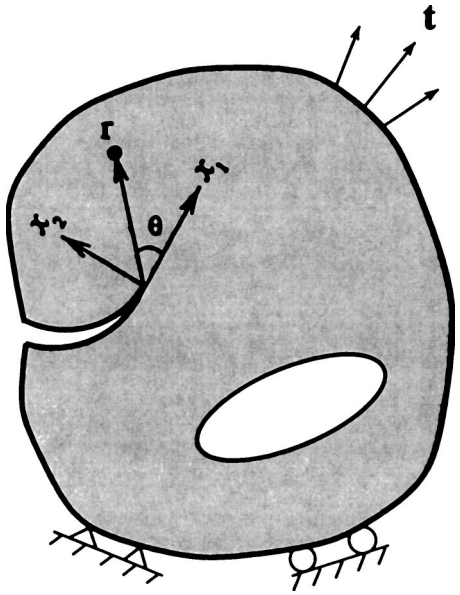

Fig. 2 Cartesian (x_1, x_2) and polar (r, θ) coordinates originating from the crack tip in a nonhomogeneous material subjected to traction (t) and displacement boundary conditions

method has been employed to evaluate T stress in isotropic [11] and orthotropic [12] FGMs. In the aforementioned papers, the interaction integral method has been investigated by means of either an *incompatibility formulation* [8–12] or a *constant-constitutive-tensor formulation* [9]. Thus, for completeness and unification of concepts, this work introduces a *nonequilibrium formulation* for evaluating SIFs and T stress in isotropic and orthotropic FGMs. These three basic formulations (see Sec. 1) will be addressed in this investigation, which includes a critical assessment and comparison of the formulations.

The FEM has been widely used for fracture of FGMs. Eischen [13] evaluated mixed-mode SIFs by means of the path-independent J_k^* integral. Gu et al. [14] evaluated SIFs using the standard J integral. Anlas et al. [15] calculated SIFs by using the path-independent J_1^* integral. Marur and Tippur [16] investigated a crack normal to the material gradient using the FEM in conjunction with experiments. Bao and Cai [17] studied delamination cracking in a graded ceramic/metal substrate under mechanical and thermal loads. Bao and Wang [18] investigated periodic cracking in graded ceramic/metal coatings under mechanical and thermal loads. Kim and Paulino [19] evaluated mixed-mode SIFs by means of the path-independent J_k^* integral, the modified crack closure (MCC), and the displacement correlation technique. Moreover, Kim and Paulino investigated mixed-mode SIFs for cracks arbitrarily oriented in orthotropic FGMs using the MCC method [20] and the path-independent J_k^* integral [21]. The nonsingular stress (T stress) of the Williams's eigenfunction expansion [22] has also been computed by means of the FEM. Becker et al. [23] studied T stress and finite crack kinking in FGMs. They calculated T stress using the difference of the normal stresses along $\theta=0$, i.e., $(\sigma_{xx}-\sigma_{yy})$. Recently, Kim and Paulino [11] proposed a unified approach using the interaction integral method to evaluate T stress and SIFs in FGMs, and also investigated the effect of T stress on crack initiation angles.

Table 1 Comparison of alternative formulations

Nonequilibrium formulation	Incompatibility formulation	Constant-constitutive-tensor formulation
$\boldsymbol{u}^{\text{aux}}$	$\boldsymbol{u}^{\text{aux}}$	$\boldsymbol{u}^{\text{aux}}$
$\boldsymbol{\varepsilon}^{\text{aux}}$	$\boldsymbol{\sigma}^{\text{aux}}$	$\boldsymbol{\varepsilon}^{\text{aux}}$
$\boldsymbol{\sigma}^{\text{aux}}=\boldsymbol{C}(\boldsymbol{x})\boldsymbol{\varepsilon}^{\text{aux}}$	$\boldsymbol{\varepsilon}^{\text{aux}}=\boldsymbol{S}(\boldsymbol{x})\boldsymbol{\sigma}^{\text{aux}}$	$\boldsymbol{\sigma}^{\text{aux}}=\boldsymbol{C}_{\text{tip}}\boldsymbol{\varepsilon}^{\text{aux}}$
$\boldsymbol{\nabla}\cdot\boldsymbol{\sigma}^{\text{aux}}\neq 0$	$\boldsymbol{\varepsilon}^{\text{aux}}\neq(\text{sym}\boldsymbol{\nabla})\boldsymbol{u}^{\text{aux}}$	$\boldsymbol{C}(\boldsymbol{x})\neq\boldsymbol{C}_{\text{tip}}$

Other methods have also been used to investigate fracture of FGMs (see the papers by Erdogan [24], Noda [25], and Paulino et al. [26]). Analytical or semi-analytical approaches have been used by Delale and Erdogan [27], Erdogan [24], Erdogan and Wu [28], and Chan et al. [29]. Delale and Erdogan [30] investigated a crack in a FGM layer between two dissimilar homogeneous half-planes. Gu and Asaro [31] studied a semi-infinite crack in a FGM strip. Shbeeb et al. [32,33] studied multiple cracks interacting in an infinite nonhomogeneous plate. Honein and Herrmann [34] studied conservation laws in nonhomogeneous plane elastostatics and investigated a semi-infinite crack by using the path-independent J_e integral. Gu and Asaro [31] studied orthotropic FGMs considering a four-point bending specimen. Ozturk and Erdogan [35,36] used integral equations to investigate mode I and mixed-mode crack problems in an infinite nonhomogeneous orthotropic medium with a crack aligned with one of the principal material directions. Due to its generality, the FEM is the method of choice in this work.

3 Auxiliary Fields

The interaction integral makes use of auxiliary fields, such as displacements ($\boldsymbol{u}^{\text{aux}}$), strains ($\boldsymbol{\varepsilon}^{\text{aux}}$), and stresses ($\boldsymbol{\sigma}^{\text{aux}}$). These auxiliary fields have to be suitably defined in order to evaluate mixed-mode SIFs and T stress. There are various choices for the auxiliary fields. Here we adopt fields originally developed for homogeneous materials. For each formulation (nonequilibrium, incompatibility, constant-constitutive tensor), the selection of auxiliary fields is done according to Table 1. The auxiliary fields adopted in this paper are described later.

3.1 Fields for SIFs. For evaluating mixed-mode SIFs, we select the auxiliary displacement, strain, and stress fields as the crack-tip asymptotic fields (i.e., $O(r^{1/2})$ for the displacements and $O(r^{-1/2})$ for the strains and stresses) with the material properties sampled at the crack-tip location (e.g., Ref. [13]): Figure 2 shows a crack in a FGM under two-dimensional fields in local Cartesian and polar coordinates originating at the crack tip. The auxiliary displacement, strain, and stress fields are chosen as [22,37]:

$$\boldsymbol{u}^{\text{aux}} = K_I^{\text{aux}}\boldsymbol{f}^{I}(r^{1/2},\theta,\boldsymbol{a}^{\text{tip}}) + K_{II}^{\text{aux}}\boldsymbol{f}^{II}(r^{1/2},\theta,\boldsymbol{a}^{\text{tip}}) \tag{1}$$

$$\boldsymbol{\varepsilon}^{\text{aux}} = (\text{sym}\,\nabla)\boldsymbol{u}^{\text{aux}}, \tag{2}$$

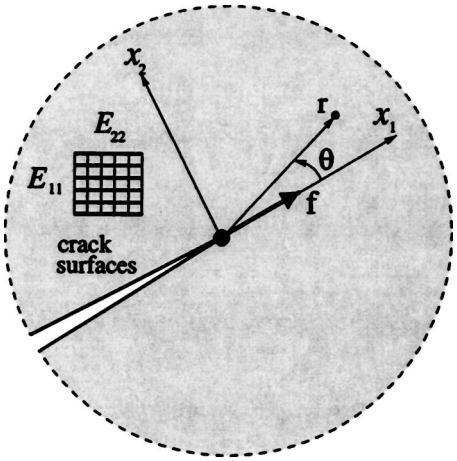

Fig. 3 A point force applied at the crack tip in the direction parallel to the crack surface

$$\boldsymbol{\sigma}^{\text{aux}} = K_I^{\text{aux}}\boldsymbol{g}^I(r^{-1/2},\theta,\boldsymbol{a}^{\text{tip}}) + K_{II}^{\text{aux}}\boldsymbol{g}^{II}(r^{-1/2},\theta,\boldsymbol{a}^{\text{tip}}) \tag{3}$$

where K_I^{aux} and K_{II}^{aux} are the auxiliary mode I and mode II SIFs, respectively, and $\boldsymbol{a}^{\text{tip}}$ denotes contracted notation of the compliance tensor $\boldsymbol{S}$ evaluated at the crack tip, which is explained in Appendix A. The representative functions $\boldsymbol{f}(r^{1/2},\theta,\boldsymbol{a}^{\text{tip}})$ and $\boldsymbol{g}(r^{-1/2},\theta,\boldsymbol{a}^{\text{tip}})$ are given in Appendix B and can also be found in other references, e.g., Refs. [37,38].

3.2 Fields for *T* stress. For evaluating T stress, we choose the auxiliary displacement, strain, and stress fields as those due to a point force in the x_1 direction, applied to the tip of a semi-infinite crack in an infinite homogeneous body as shown in Fig. 3. The auxiliary displacements, strains, and stresses are chosen as [39–41]:

$$\boldsymbol{u}^{\text{aux}} = \boldsymbol{t}^u(\ln r,\theta,f,\boldsymbol{a}^{\text{tip}}) \tag{4}$$

$$\boldsymbol{\varepsilon}^{\text{aux}} = (\text{sym}\,\nabla)\boldsymbol{u}^{\text{aux}} \tag{5}$$

$$\boldsymbol{\sigma}^{\text{aux}} = \boldsymbol{t}^s(r^{-1},\theta,f,\boldsymbol{a}^{\text{tip}}) \tag{6}$$

where f is the point force applied to the crack tip, and $\boldsymbol{a}^{\text{tip}}$ denotes contracted notation of the compliance tensor $\boldsymbol{S}$ evaluated at the crack tip, which is defined in Appendix A. The representative functions $\boldsymbol{t}^u(\ln r,\theta,f,\boldsymbol{a}^{\text{tip}})$ and $\boldsymbol{t}^s(r^{-1},\theta,f,\boldsymbol{a}^{\text{tip}})$ are given in Appendix C and can be found in other references, e.g., Refs. [39,41].

For orthotropic materials, the auxiliary fields may be determined by either the Lekhnitskii or Stroh formalism [12]. There is no difficulty in determining the auxiliary fields in the case of isotropic materials [11].

4 *M*-integral formulations

The standard J integral [42] is given by

$$J = \lim_{\Gamma_s\to 0}\int_{\Gamma_s}(\mathcal{W}\delta_{1j} - \sigma_{ij}u_{i,1})n_j d\Gamma \tag{7}$$

where $\mathcal{W}$ is the strain energy density expressed by

$$\mathcal{W} = \tfrac{1}{2}\sigma_{ij}\varepsilon_{ij} = \tfrac{1}{2}C_{ijkl}\varepsilon_{kl}\varepsilon_{ij} \tag{8}$$

and n_j is the outward normal vector to the contour Γ_s, as shown in Fig. 4. The portion of Γ with applied displacements is denoted Γ_u, and the portion of Γ with applied traction is denoted Γ_τ. Moreover $\Gamma=\Gamma_u+\Gamma_\tau$. Using a plateau-type weight function varying from $q=1$ on Γ_s to $q=0$ on Γ_0 [10] and assuming that the crack faces are traction-free, Eq. (7) becomes

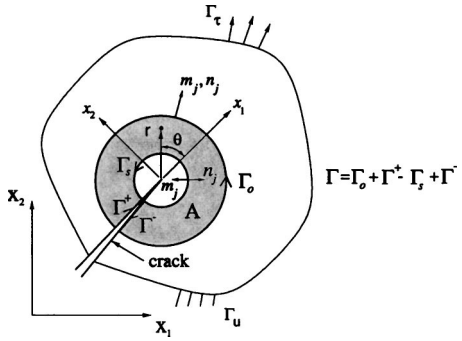

Fig. 4 Conversion of the contour integral into an EDI where $\Gamma=\Gamma_0+\Gamma^+-\Gamma_s+\Gamma^-$, $m_j=n_j$ on Γ_0 and $m_j=-n_j$ on Γ_s

$$J = \lim_{\Gamma_s\to 0}\oint_{\Gamma}(\sigma_{ij}u_{i,1} - \mathcal{W}\delta_{1j})m_j q d\Gamma \tag{9}$$

Applying the divergence theorem to Eq. (9), the equivalent domain integral (EDI) is obtained as

$$J = \int_A(\sigma_{ij}u_{i,1} - \mathcal{W}\delta_{1j})q_{,j}dA + \int_A(\sigma_{ij}u_{i,1} - \mathcal{W}\delta_{1j})_{,j}qdA \tag{10}$$

The J integral of the superimposed fields (actual and auxiliary fields) is obtained as

$$\begin{aligned} J^s = &\int_A\left\{(\sigma_{ij}+\sigma_{ij}^{\text{aux}})(u_{i,1}+u_{i,1}^{\text{aux}}) - \tfrac{1}{2}(\sigma_{ik}+\sigma_{ik}^{\text{aux}})(\varepsilon_{ik}+\varepsilon_{ik}^{\text{aux}})\delta_{1j}\right\}q_{,j}dA \\ &+\int_A\left\{(\sigma_{ij}+\sigma_{ij}^{\text{aux}})(u_{i,1}+u_{i,1}^{\text{aux}}) - \tfrac{1}{2}(\sigma_{ik}+\sigma_{ik}^{\text{aux}})(\varepsilon_{ik}+\varepsilon_{ik}^{\text{aux}})\right. \\ &\left.\times(\delta_{1j})\right\}_{,j}qdA \end{aligned} \tag{11}$$

which is conveniently decomposed into

$$J^s = J + J^{\text{aux}} + M \tag{12}$$

where J^{aux} is given by

$$\begin{aligned} J^{\text{aux}} = &\int_A(\sigma_{ij}^{\text{aux}}u_{i,1}^{\text{aux}} - \mathcal{W}^{\text{aux}}\delta_{1j})q_{,j}dA + \int_A\left\{\sigma_{ij}^{\text{aux}}u_{i,1}^{\text{aux}}\right. \\ &\left.-\tfrac{1}{2}\sigma_{ik}^{\text{aux}}\varepsilon_{ik}^{\text{aux}}\delta_{1j}\right\}_{,j}qdA \end{aligned}$$

and the resulting interaction integral (M) is given by

$$\begin{aligned} M = &\int_A\left\{\sigma_{ij}u_{i,1}^{\text{aux}} + \sigma_{ij}^{\text{aux}}u_{i,1} - \tfrac{1}{2}(\sigma_{ik}\varepsilon_{ik}^{\text{aux}} + \sigma_{ik}^{\text{aux}}\varepsilon_{ik})\delta_{1j}\right\}q_{,j}dA \\ &+\int_A\left\{\sigma_{ij}u_{i,1}^{\text{aux}} + \sigma_{ij}^{\text{aux}}u_{i,1} - \tfrac{1}{2}(\sigma_{ik}\varepsilon_{ik}^{\text{aux}} + \sigma_{ik}^{\text{aux}}\varepsilon_{ik})\delta_{1j}\right\}_{,j}qdA \end{aligned} \tag{13}$$

This general form of M integral becomes a specific form of M integral for each of the three formulations, which is explained in the next section.

4.1 Nonequilibrium Formulation. The name of the formulation is based on the fact that the auxiliary stress field

$$\sigma_{ij}^{\text{aux}} = C_{ijkl}(\boldsymbol{x})\varepsilon_{kl}^{\text{aux}} \tag{14}$$

does not satisfy equilibrium because it differs from

$$\sigma_{ij}^{\text{aux}} = (C_{ijkl})_{\text{tip}} \varepsilon_{kl}^{\text{aux}}, \tag{15}$$

where $C_{ijkl}(\boldsymbol{x})$ is the constitutive tensor of the actual FGM and $(C_{ijkl})_{\text{tip}}$ is the constitutive tensor at the crack tip (see Fig. 1). The derivatives of the auxiliary stress field are

$$\sigma_{ij,j}^{\text{aux}} = C_{ijkl,j}(\boldsymbol{x})\varepsilon_{kl}^{\text{aux}} + C_{ijkl}(\boldsymbol{x})\varepsilon_{kl,j}^{\text{aux}} = \underline{(C_{ijkl})_{\text{tip}}\varepsilon_{kl,j}^{\text{aux}}} + C_{ijkl,j}(\boldsymbol{x})\varepsilon_{kl}^{\text{aux}} + [C_{ijkl}(\boldsymbol{x}) - (C_{ijkl})_{\text{tip}}]\varepsilon_{kl,j}^{\text{aux}}, \tag{16}$$

where the underlined term in Eq. (16) vanishes. Thus this argument confirms that the auxiliary stress field selected in this formulation (Eq. (14)) does not satisfy equilibrium, i.e., $\sigma_{ij,j}^{\text{aux}} \neq 0$ (no body forces or inertia). This choice of the auxiliary fields has been discussed by Dolbow and Gosz [8], but a nonequilibrium formulation was not provided in their paper. The nonequilibrium in the stress field has to be taken into account in the interaction integral formulation, which is discussed in detail later.

Using the following equality:

$$\sigma_{ij}\varepsilon_{ij}^{\text{aux}} = C_{ijkl}(\boldsymbol{x})\varepsilon_{kl}\varepsilon_{ij}^{\text{aux}} = \sigma_{kl}^{\text{aux}}\varepsilon_{kl} = \sigma_{ij}^{\text{aux}}\varepsilon_{ij} \tag{17}$$

one rewrites Eq. (13) as

$$M = \int_A \{\sigma_{ij}u_{i,1}^{\text{aux}} + \sigma_{ij}^{\text{aux}}u_{i,1} - \sigma_{ik}\varepsilon_{ik}^{\text{aux}}\delta_{1j}\}q_{,j}dA + \int_A \{\sigma_{ij}u_{i,1}^{\text{aux}} + \sigma_{ij}^{\text{aux}}u_{i,1} - \sigma_{ik}\varepsilon_{ik}^{\text{aux}}\delta_{1j}\}_{,j}qdA = M_1 + M_2 \tag{18}$$

The last term of the second integral (M_2) in Eq. (18) is expressed as

$$\begin{aligned}(\sigma_{ik}\varepsilon_{ik}^{\text{aux}}\delta_{1j})_{,j} &= (\sigma_{ik}\varepsilon_{ik}^{\text{aux}})_{,1} = (\sigma_{ij}\varepsilon_{ij}^{\text{aux}})_{,1} = (C_{ijkl}\varepsilon_{kl}\varepsilon_{ij}^{\text{aux}})_{,1} \\ &= C_{ijkl,1}\varepsilon_{kl}\varepsilon_{ij}^{\text{aux}} + C_{ijkl}\varepsilon_{kl,1}\varepsilon_{ij}^{\text{aux}} + C_{ijkl}\varepsilon_{kl}\varepsilon_{ij,1}^{\text{aux}} \\ &= C_{ijkl,1}\varepsilon_{kl}\varepsilon_{ij}^{\text{aux}} + \sigma_{ij}^{\text{aux}}\varepsilon_{ij,1} + \sigma_{ij}\varepsilon_{ij,1}^{\text{aux}}\end{aligned} \tag{19}$$

Substitution of Eq. (19) into Eq. (18) leads to

$$M_2 = \int_A (\sigma_{ij,j}u_{i,1}^{\text{aux}} + \sigma_{ij}u_{i,1j}^{\text{aux}} + \sigma_{ij,j}^{\text{aux}}u_{i,1} + \sigma_{ij}^{\text{aux}}u_{i,1j})qdA - \int_A (C_{ijkl,1}\varepsilon_{kl}\varepsilon_{ij}^{\text{aux}} + \sigma_{ij}^{\text{aux}}\varepsilon_{ij,1} + \sigma_{ij}\varepsilon_{ij,1}^{\text{aux}})qdA \tag{20}$$

Using compatibility (actual and auxiliary) and equilibrium (actual) (i.e., $\sigma_{ij,j}=0$ with no body force), one simplifies Eq. (20) as

$$M_2 = \int_A \{\sigma_{ij,j}^{\text{aux}}u_{i,1} - C_{ijkl,1}\varepsilon_{kl}\varepsilon_{ij}^{\text{aux}}\}qdA \tag{21}$$

Therefore the resulting interaction integral (M) becomes

$$M = \int_A \{\sigma_{ij}u_{i,1}^{\text{aux}} + \sigma_{ij}^{\text{aux}}u_{i,1} - \sigma_{ik}\varepsilon_{ik}^{\text{aux}}\delta_{1j}\}q_{,j}dA + \int_A \{\underline{\sigma_{ij,j}^{\text{aux}}u_{i,1}} - C_{ijkl,1}\varepsilon_{kl}\varepsilon_{ij}^{\text{aux}}\}qdA \tag{22}$$

where the underlined term is a nonequilibrium term, which appears due to nonequilibrium of the auxiliary stress fields. The existence of the final form of M integral for FGMs in Eq. (22) has been proved by Kim [43] and Paulino and Kim [44].

4.2 Incompatibilty Formulation. The incompatibility formulation satisfies equilibrium ($\sigma_{ij,j}^{\text{aux}}=0$ with no body forces) and the constitutive relationship ($\varepsilon_{ij}^{\text{aux}}=S_{ijkl}(\boldsymbol{x})\sigma_{kl}^{\text{aux}}$), but violates compatiblity conditions ($\varepsilon_{ij}^{\text{aux}} \neq (u_{i,j}^{\text{aux}}+u_{j,i}^{\text{aux}})/2$). Thus Eq. (20) is also valid for this formulation. Using equilibrium (actual and auxiliary) and compatibility (actual), one simplifies M_2 as

$$M_2 = \int_A \{\sigma_{ij}(u_{i,1j}^{\text{aux}} - \varepsilon_{ij,1}^{\text{aux}}) - C_{ijkl,1}\varepsilon_{kl}\varepsilon_{ij}^{\text{aux}}\}qdA$$

Therefore the resulting interaction integral (M) becomes

$$M = \int_A \{\sigma_{ij}u_{i,1}^{\text{aux}} + \sigma_{ij}^{\text{aux}}u_{i,1} - \sigma_{ik}\varepsilon_{ik}^{\text{aux}}\delta_{1j}\}q_{,j}dA + \int_A \{\underline{\sigma_{ij}(u_{i,1j}^{\text{aux}} - \varepsilon_{ij,1}^{\text{aux}})} - C_{ijkl,1}\varepsilon_{kl}\varepsilon_{ij}^{\text{aux}}\}qdA \tag{23}$$

where the underlined term is an incompatibility term, which appears due to incompatibility of the auxiliary strain fields. The existence of the final form of M integral for FGMs in Eq. (23) has been proved by Kim [43].

4.3 Constant-Constitutive-Tensor Formulation. The constant-constitutive-tensor formulation satisfies equilibrium ($\sigma_{ij,j}^{\text{aux}}=0$ with no body forces) and compatiblity conditions ($\varepsilon_{ij}^{\text{aux}}=(u_{i,j}^{\text{aux}}+u_{j,i}^{\text{aux}})/2$), but violates the constitutive relationship ($\sigma_{ij}^{\text{aux}}=(C_{ijkl})_{\text{tip}}\varepsilon_{kl}^{\text{aux}}$ with $(C_{ijkl})_{\text{tip}} \neq C_{ijkl}(\boldsymbol{x})$). Notice that $\sigma_{ij}\varepsilon_{ij}^{\text{aux}} \neq \sigma_{ij}^{\text{aux}}\varepsilon_{ij}$ due to the violated constitutive relationship. Thus Eq. (13) becomes

$$\begin{aligned}M = &\int_A \left\{\sigma_{ij}u_{i,1}^{\text{aux}} + \sigma_{ij}^{\text{aux}}u_{i,1} - \tfrac{1}{2}(\sigma_{ik}\varepsilon_{ik}^{\text{aux}} + \sigma_{ik}^{\text{aux}}\varepsilon_{ik})\delta_{1j}\right\}q_{,j}dA \\ &+ \int_A \left\{\sigma_{ij,j}u_{i,1}^{\text{aux}} + \sigma_{ij}u_{i,1j}^{\text{aux}} + \sigma_{ij,j}^{\text{aux}}u_{i,1} + \sigma_{ij}^{\text{aux}}u_{i,1j} - \tfrac{1}{2}(\sigma_{ij,1}\varepsilon_{ij}^{\text{aux}} \right. \\ &\left. + \sigma_{ij}\varepsilon_{ij,1}^{\text{aux}} + \sigma_{ij,1}^{\text{aux}}\varepsilon_{ij} + \sigma_{ij}^{\text{aux}}\varepsilon_{ij,1})\right\}qdA\end{aligned} \tag{24}$$

Using equilibrium and compatibility conditions for both actual and auxiliary fields, one obtains M as

$$M = \int_A \left\{\sigma_{ij}u_{i,1}^{\text{aux}} + \sigma_{ij}^{\text{aux}}u_{i,1} - \tfrac{1}{2}(\sigma_{ik}\varepsilon_{ik}^{\text{aux}} + \sigma_{ik}^{\text{aux}}\varepsilon_{ik})\delta_{1j}\right\}q_{,j}dA + \int_A \tfrac{1}{2}\{\sigma_{ij}\varepsilon_{ij,1}^{\text{aux}} - \sigma_{ij,1}\varepsilon_{ij}^{\text{aux}} + \sigma_{ij}^{\text{aux}}\varepsilon_{ij,1} - \sigma_{ij,1}^{\text{aux}}\varepsilon_{ij}\}qdA \tag{25}$$

Notice that the resulting M involves derivatives of the actual strain and stress fields, which arises due to the material mismatch, and may cause loss of accuracy from a numerical point of view. The existence of the final form of M integral for FGMs in Eq. (25) has been proved by Kim [43].

5 Extraction of Stress Intensity Factors

For mixed-mode crack problems on orthotropic materials, the energy release rates $\mathcal{G}_I$ and $\mathcal{G}_{II}$ are related to mixed-mode SIFs as follows [37]:

$$\mathcal{G}_I = -\frac{K_I}{2}a_{22}^{\text{tip}}\,\text{Im}\left[\frac{K_I(\mu_1^{\text{tip}}+\mu_2^{\text{tip}}) + K_{II}}{\mu_1^{\text{tip}}\mu_2^{\text{tip}}}\right] \tag{26}$$

$$\mathcal{G}_{II} = \frac{K_{II}}{2}a_{11}^{\text{tip}}\,\text{Im}[K_{II}(\mu_1^{\text{tip}}+\mu_2^{\text{tip}}) + K_I(\mu_1^{\text{tip}}\mu_2^{\text{tip}})] \tag{27}$$

where Im denotes the imaginary part of the complex function. Thus

$$J_{\text{local}} = \mathcal{G} = \mathcal{G}_I + \mathcal{G}_{II} = c_{11}K_I^2 + c_{12}K_IK_{II} + c_{22}K_{II}^2 \tag{28}$$

where

$$\begin{aligned}c_{11} &= -\frac{a_{22}^{\text{tip}}}{2}\,\text{Im}\left(\frac{\mu_1^{\text{tip}}+\mu_2^{\text{tip}}}{\mu_1^{\text{tip}}\mu_2^{\text{tip}}}\right) \\ c_{12} &= -\frac{a_{22}^{\text{tip}}}{2}\,\text{Im}\left(\frac{1}{\mu_1^{\text{tip}}\mu_2^{\text{tip}}}\right) + \frac{a_{11}^{\text{tip}}}{2}\,\text{Im}(\mu_1^{\text{tip}}\mu_2^{\text{tip}}) \\ c_{22} &= \frac{a_{11}^{\text{tip}}}{2}\,\text{Im}(\mu_1^{\text{tip}}+\mu_2^{\text{tip}})\end{aligned} \tag{29}$$

For two admissible fields, which are the actual ($\boldsymbol{u}, \boldsymbol{\varepsilon}, \boldsymbol{\sigma}$) and auxiliary ($\boldsymbol{u}^{\text{aux}}, \boldsymbol{\varepsilon}^{\text{aux}}, \boldsymbol{\sigma}^{\text{aux}}$) fields, one obtains [6]:

$$J^s_{\text{local}} = c_{11}(K_I + K_I^{\text{aux}})^2 + c_{12}(K_I + K_I^{\text{aux}})(K_{II} + K_{II}^{\text{aux}}) + c_{22}(K_{II} + K_{II}^{\text{aux}})^2 = J_{\text{local}} + J^{\text{aux}}_{\text{local}} + M_{\text{local}} \tag{30}$$

where J_{local} is given by Eq. (28), $J^{\text{aux}}_{\text{local}}$ is given by

$$J^{\text{aux}}_{\text{local}} = c_{11}(K_I^{\text{aux}})^2 + c_{12}K_I^{\text{aux}}K_{II}^{\text{aux}} + c_{22}(K_{II}^{\text{aux}})^2 \tag{31}$$

and M_{local} is given by

$$M_{\text{local}} = 2c_{11}K_IK_I^{\text{aux}} + c_{12}(K_IK_{II}^{\text{aux}} + K_I^{\text{aux}}K_{II}) + 2c_{22}K_{II}K_{II}^{\text{aux}} \tag{32}$$

The mode I and mode II SIFs are evaluated by solving the following linear algebraic equations:

$$M^{(1)}_{\text{local}} = 2c_{11}K_I + c_{12}K_{II}, \quad (K_I^{\text{aux}} = 1.0, K_{II}^{\text{aux}} = 0.0) \tag{33}$$

$$M^{(2)}_{\text{local}} = c_{12}K_I + 2c_{22}K_{II}, \quad (K_I^{\text{aux}} = 0.0, K_{II}^{\text{aux}} = 1.0) \tag{34}$$

where the superscript in $M^{(i)}_{\text{local}}$ $(i=1,2)$ is used just to indicate that the values are distinct in each case. For isotropic materials, the off-diagonal terms of c_{ij} drop, and Eqs. (33) and (34) become

$$M^{(1)}_{\text{local}} = \frac{2}{E^*_{\text{tip}}}K_I \quad (K_I^{\text{aux}} = 1.0, K_{II}^{\text{aux}} = 0.0) \tag{35}$$

$$M^{(2)}_{\text{local}} = \frac{2}{E^*_{\text{tip}}}K_{II}, \quad (K_I^{\text{aux}} = 0.0, K_{II}^{\text{aux}} = 1.0) \tag{36}$$

respectively, where $E^*_{\text{tip}} = E_{\text{tip}}$ for plane stress and $E^*_{\text{tip}} = E_{\text{tip}}/(1-\nu^2_{\text{tip}})$ for plane strain. The relationships of Eqs. (33) and (34), and Eqs. (35) and (36) are the same as those for homogeneous orthotropic [6] and isotropic [5] materials, respectively, except that, for FGMs, the material properties are evaluated at the crack-tip location. Notice that, for the orthotropic case, there is no need for Newton's iteration, which is needed with other approaches such as the path-independent J_k integral [21] and the MCC integral [20]. Here the SIFs for mode I and mode II are naturally decoupled (cf. Eqs. (33) and (34)).

6 Extraction of *T* Stress

T stress can be extracted from the interaction integral by nullifying the contributions of both singular (i.e., $O(r^{-1/2})$) and higher-order (i.e., $O(r^{1/2})$ and higher) terms. The derivation is explained in detail by Kim and Paulino [11,12] and Paulino and Kim [44]. From the earlier derivation of Eq. (13), the *M* integral in the form of line integral is obtained as

$$M_{\text{local}} = \lim_{\Gamma_s \to 0} \int_{\Gamma_s} \{\sigma_{ik}\varepsilon^{\text{aux}}_{ik}\delta_{1j} - \sigma_{ij}u^{\text{aux}}_{i,1} - \sigma^{\text{aux}}_{ij}u_{i,1}\}n_j d\Gamma \tag{37}$$

Here we can consider only the stress parallel to the crack direction, i.e.:

$$\sigma_{ij} = T\delta_{1i}\delta_{1j} \tag{38}$$

Substituting Eq. (38) into Eq. (37), one obtains

$$M_{\text{local}} = -\lim_{\Gamma_s \to 0} \int_{\Gamma_s} \sigma^{\text{aux}}_{ij}n_j u_{i,1} d\Gamma = Ta^{\text{tip}}_{11} \lim_{\Gamma_s \to 0} \int_{\Gamma_s} \sigma^{\text{aux}}_{ij}n_j d\Gamma \tag{39}$$

Because the force f is in equilibrium (see Fig. 3):

$$f = -\lim_{\Gamma_s \to 0} \int_{\Gamma_s} \sigma^{\text{aux}}_{ij}n_j d\Gamma \tag{40}$$

and thus the following relationship is obtained:

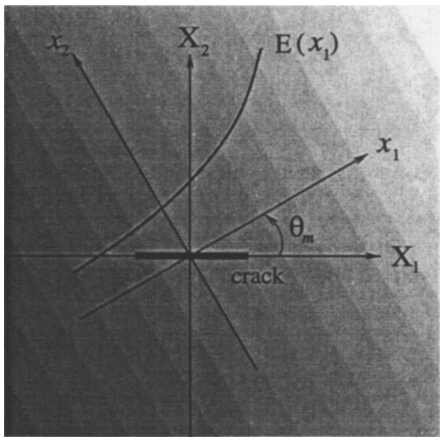

Fig. 5 Crack geometry in a nonhomogeneous material, which is graded along the x_1 direction

$$T = \frac{M_{\text{local}}}{fa^{\text{tip}}_{11}} \tag{41}$$

where a^{tip}_{11} is a material parameter at the crack tip location for plane stress, and is replaced by b^{tip}_{11} for plane strain (cf. Eq. (65)). For isotropic materials, Eq. (41) becomes

$$T = \frac{E^*_{\text{tip}}}{f}M_{\text{local}} \tag{42}$$

where $E^*_{\text{tip}} = E_{\text{tip}}$ for plane stress and $E^*_{\text{tip}} = E_{\text{tip}}/(1-\nu^2_{\text{tip}})$ for plane strain.

7 Comparison and Critical Assessment

The three formulations presented earlier are *consistent* in the sense that extra terms are added to account for the difference in response between homogeneous and nonhomogeneous materials. However, each formulation has an independent final form (see Eqs. (22), (23), and (25)) due to the different characteristics of the auxiliary fields. The final form of the *M* integral for each of these formulations is compared and assessed from a theoretical point of view later.

The nonequilibrium formulation results in the simplest final *M* integral thus requiring the least computation and implementation effort among the three formulations. This is observed by comparing Eqs. (22), (23), and (25). Moreover, the nonequilibrium formulation is equivalent to the incompatibility formulation, because both formulations involve the same constitutive relations and corresponding material derivatives. This equivalence is observed in the numerical examples of Sec. 9. However, the constant-constitutive-tensor formulation [9] requires the derivatives of the actual stress field, which may introduce accuracy problems with standard C^0 elements commonly used in the displacement-based FEM.

In order to further compare the three consistent formulations, let's consider an exponentially graded material in which Poisson's ratio is constant and Young's modulus varies in any direction (see Fig. 5):

$$E(x_1) = E_0 \exp(\delta x_1) = E_0 \exp(\beta_1 X_1 + \beta_2 X_2) \tag{43}$$

$$\nu = \text{constant} \tag{44}$$

where $\boldsymbol{X} = (X_1, X_2)$ refers to a global coordinate system, x_1 is the direction of material gradation (inclined by θ_m with respect to the X_1 coordinate), and the nonhomogeneity parameters δ, β_1, and β_2 are related by

$$\beta_1 = \delta \cos\theta_m, \quad \beta_2 = \delta \sin\theta_m \tag{45}$$

This selection of material property leads to simplification of the resulting M integrals and allows one to better assess and compare the characteristics of the formulations. Moreover, exponentially graded materials have been extensively investigated in the technical literature, e.g., Refs. [8,15,19,21,24,27–36,45–48]. The resulting M integrals corresponding to the three formulations are derived later in the global coordinate system, which is used in the numerical implementation (see Sec. 8 later).

7.1 Nonequilibrium Formulation. The derivatives of interest, with respect to the global coordinate system, are $(m=1,2)$

$$\sigma^{\text{aux}}_{ij,j} = C_{ijkl,j}(\boldsymbol{X})\varepsilon^{\text{aux}}_{kl} + C_{ijkl}(\boldsymbol{X})\varepsilon^{\text{aux}}_{kl,j} = \beta_j C_{ijkl}(\boldsymbol{X})\varepsilon^{\text{aux}}_{kl} + C_{ijkl}(\boldsymbol{X})\varepsilon^{\text{aux}}_{kl,j} = \beta_j C_{ijkl}(\boldsymbol{X})\varepsilon^{\text{aux}}_{kl} + \alpha_p (C_{ijkl})_{\text{tip}}\varepsilon^{\text{aux}}_{kl,j} = \beta_j \sigma^{\text{aux}}_{ij} \tag{46}$$

$$C_{ijkl,m} = \beta_m C_{ijkl}(\boldsymbol{X}) \tag{47}$$

where $\alpha_p = \exp(\beta_1 X_1 + \beta_2 X_2)$ is a factor that arises due to the proportionality of C_{ijkl} for the material gradation considered. The global interaction integral $(M_m)_{\text{global}}$ $(m=1,2)$ is given by

$$(M_m)_{\text{global}} = \int_A \{\sigma_{ij} u^{\text{aux}}_{i,m} + \sigma^{\text{aux}}_{ij} u_{i,m} - \sigma_{ik}\varepsilon^{\text{aux}}_{ik}\delta_{1j}\}\frac{\partial q}{\partial X_j} dA + \int_A \{\sigma^{\text{aux}}_{ij,j} u_{i,m} - C_{ijkl,m}\varepsilon_{kl}\varepsilon^{\text{aux}}_{ij}\} q dA \tag{48}$$

Substitution of Eqs. (46) and (47) into Eq. (48) yields $(m=1,2)$:

$$(M_m)_{\text{global}} = \int_A \{\sigma_{ij} u^{\text{aux}}_{i,m} + \sigma^{\text{aux}}_{ij} u_{i,m} - \sigma_{ik}\varepsilon^{\text{aux}}_{ik}\delta_{mj}\}\frac{\partial q}{\partial X_j} dA + \int_A \{\beta_j \sigma^{\text{aux}}_{ij} u_{i,m} - \beta_m \sigma_{ij}\varepsilon^{\text{aux}}_{ij}\} q dA \tag{49}$$

Notice that, for this particular case, a simpler expression than that for the general case is obtained (cf. Eq. (22)). The derivatives of material properties are represented by the material nonhomogeneity β in Eq. (49). Moreover, the contribution of the nonequilibrium term to the M integral is related to the value of β.

7.2 Incompatibility Formulation. The derivatives of interest, with respect to the global coordinate system, are $(m=1,2)$:

$$\varepsilon^{\text{aux}}_{ij,m} = S_{ijkl,m}(\boldsymbol{X})\sigma^{\text{aux}}_{kl} + S_{ijkl}(\boldsymbol{X})\sigma^{\text{aux}}_{kl,m} = -\beta_m S_{ijkl}(\boldsymbol{X})\sigma^{\text{aux}}_{kl} + S_{ijkl}(\boldsymbol{X})\sigma^{\text{aux}}_{kl,m} = -\beta_m \varepsilon^{\text{aux}}_{ij} + S_{ijkl}(\boldsymbol{X})\sigma^{\text{aux}}_{kl,m} \tag{50}$$

together with Eq. (47). The global interaction integral $(M_m)_{\text{global}}$ $(m=1,2)$ is given by

$$(M_m)_{\text{global}} = \int_A \{\sigma_{ij} u^{\text{aux}}_{i,m} + \sigma^{\text{aux}}_{ij} u_{i,m} - \sigma_{ik}\varepsilon^{\text{aux}}_{ik}\delta_{mj}\}\frac{\partial q}{\partial X_j} dA + \int_A \{\sigma_{ij}(u^{\text{aux}}_{i,mj} - \varepsilon^{\text{aux}}_{ij,m}) - C_{ijkl,m}\varepsilon_{kl}\varepsilon^{\text{aux}}_{ij}\} q dA \tag{51}$$

Substitution of Eqs. (50) and (47) into Eq. (51) yields $(m=1,2)$:

$$(M_m)_{\text{global}} = \int_A \{\sigma_{ij} u^{\text{aux}}_{i,m} + \sigma^{\text{aux}}_{ij} u_{i,m} - \sigma_{ik}\varepsilon^{\text{aux}}_{ik}\delta_{mj}\}\frac{\partial q}{\partial X_j} dA + \int_A \{\sigma_{ij} u^{\text{aux}}_{i,mj} - \sigma^{\text{aux}}_{ij,m}\varepsilon_{ij}\} q dA \tag{52}$$

Notice that, for this particular case, the final M integral does not involve any derivatives of material properties (cf. Eq. (23)). In this formulation, the first integral of Eq. (52) is the same as that for the nonequilibrium formulation, because both formulations use the same constitutive tensor $\boldsymbol{C}(\boldsymbol{X})$.

7.3 Constant-Constitutive-Tensor Formulation. The derivatives of interest, with respect to the global coordinate system, are $(m=1,2)$:

$$\sigma_{ij,m} = C_{ijkl,m}(\boldsymbol{X})\varepsilon_{kl} + C_{ijkl}(\boldsymbol{X})\varepsilon_{kl,m} = \beta_m C_{ijkl}(\boldsymbol{X})\varepsilon_{kl} + C_{ijkl}(\boldsymbol{X})\varepsilon_{kl,m} = \beta_m \sigma_{ij} + C_{ijkl}(\boldsymbol{X})\varepsilon_{kl,m} \tag{53}$$

$$\sigma^{\text{aux}}_{ij,m} = (C_{ijkl})_{\text{tip}}\varepsilon^{\text{aux}}_{kl,m} \tag{54}$$

The global interaction integral $(M_m)_{\text{global}}$ $(m=1,2)$ is given by

$$M = \int_A \left\{\sigma_{ij} u^{\text{aux}}_{i,m} + \sigma^{\text{aux}}_{ij} u_{i,m} - \frac{1}{2}(\sigma_{ik}\varepsilon^{\text{aux}}_{ik} + \sigma^{\text{aux}}_{ik}\varepsilon_{ik})\delta_{mj}\right\}\frac{\partial q}{\partial X_j} dA + \int_A \frac{1}{2}\{\sigma_{ij}\varepsilon^{\text{aux}}_{ij,m} - \sigma_{ij,m}\varepsilon^{\text{aux}}_{ij} + \sigma^{\text{aux}}_{ij}\varepsilon_{ij,m} - \sigma^{\text{aux}}_{ij,m}\varepsilon_{ij}\} q dA \tag{55}$$

Substitution of Eqs. (53) and (54) into Eq. (55) yields $(m=1,2)$:

$$M = \int_A \left\{\sigma_{ij} u^{\text{aux}}_{i,m} + \sigma^{\text{aux}}_{ij} u_{i,m} - \frac{1}{2}(\sigma_{ik}\varepsilon^{\text{aux}}_{ik} + \sigma^{\text{aux}}_{ik}\varepsilon_{ik})\delta_{mj}\right\}\frac{\partial q}{\partial X_j} dA + \int_A \frac{1}{2}\{\sigma_{ij}\varepsilon^{\text{aux}}_{ij,m} - \beta_m \sigma_{ij}\varepsilon^{\text{aux}}_{ij} - C_{ijkl}\varepsilon_{kl,m}\varepsilon^{\text{aux}}_{ij} + \sigma^{\text{aux}}_{ij}\varepsilon_{ij,m} - (C_{ijkl})_{\text{tip}}\varepsilon^{\text{aux}}_{kl,m}\varepsilon_{ij}\} q dA \tag{56}$$

where $C_{ijkl} \equiv C_{ijkl}(\boldsymbol{X})$. Notice that, for this case, the final M integral requires the derivatives of the actual strain field, which may have numerical accuracy problems. The derivatives of material properties are represented by the material nonhomogeneity β in Eq. (56). Moreover, the first integral of Eq. (56) is different from those for the other two formulations.

8 Some Numerical Aspects

For numerical computation by means of the FEM, the M integral is evaluated first in global coordinates ($(M_m)_{\text{global}}$) and then transformed to local coordinates (M_{local}). The M integrals $(M_m)_{\text{global}}$ for the three consistent formulations have derivatives of material properties in common. In this paper, we do not use closed-form expressions for derivatives of material properties because these expressions would be specific to each specific function or micromechanics model. Thus, for the sake of generality, we determine such derivatives by using shape function derivatives of finite elements [19,45].

The derivatives involving material derivatives for each formulation are

- nonequilibrium: $\sigma^{\text{aux}}_{ij,j} = C_{ijkl,j}\varepsilon^{\text{aux}}_{kl} + C_{ijkl}\varepsilon^{\text{aux}}_{kl,j}$ (57)
- incompatibility: $\varepsilon^{\text{aux}}_{ij,m} = S_{ijkl,m}\sigma^{\text{aux}}_{kl} + S_{ijkl}\sigma^{\text{aux}}_{kl,m}$ (58)
- constant-constitutive-tensor: $\sigma_{ij,m} = C_{ijkl,m}\varepsilon_{kl} + C_{ijkl}\varepsilon_{kl,m}$ (59)

A simple and general approach to evaluate such derivatives consists of using shape function derivatives [11]. Thus the derivatives of a generic quantity P (e.g., C_{ijkl}, S_{ijkl}, or ε_{ij}) are obtained as

$$\frac{\partial P}{\partial X_m} = \sum_{i=1}^{n} \frac{\partial N_i}{\partial X_m} P_i, \quad (m=1,2) \tag{60}$$

where n is the number of element nodes and $N_i = N_i(\xi,\eta)$ are the element shape functions which can be found in many references, e.g., Ref. [49]. The derivatives $\partial N_i / \partial X_m$ are obtained as

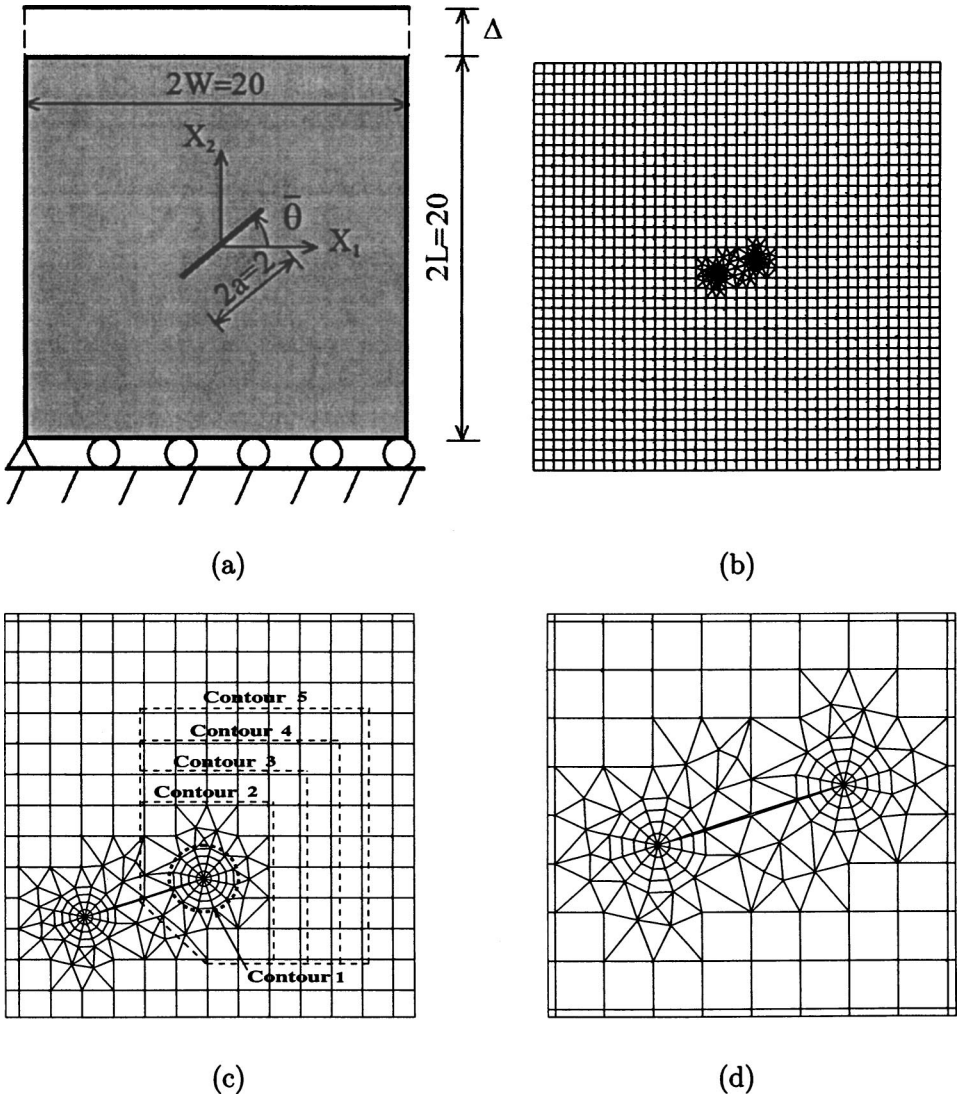

Fig. 6 Example 1: FGM plate with an inclined crack with geometric angle $\bar{\theta}$: (*a*) geometry and boundary conditions (BCs) under fixed-grip loading; (*b*) typical finite element mesh; (*c*) contours for EDI computation of *M* integral; (*d*) mesh detail using 12 sectors (*S*12) and four rings (*R*4) around the crack tips (θ=18° counter-clockwise)

$$\begin{Bmatrix} \partial N_i/\partial X_1 \\ \partial N_i/\partial X_2 \end{Bmatrix} = \boldsymbol{J}^{-1} \begin{Bmatrix} \partial N_i/\partial \xi \\ \partial N_i/\partial \eta \end{Bmatrix} \tag{61}$$

where $\boldsymbol{J}^{-1}$ is the inverse of the standard Jacobian matrix relating (X_1, X_2) with (ξ, η) [49].

9 Numerical Examples

The performance of the interaction integral for evaluating SIFs and *T* stress in isotropic and orthotropic FGMs is examined by means of numerical examples. This paper employs the three formulations, such as nonequilibrium, incompatibility, and constant-constitutive tensor, for numerical investigation. The following examples are presented

(1) Inclined center crack in a plate
(2) Strip with an edge crack

All the examples are analyzed using the FEM code I-FRANC2D[4]. (Illinois; FRacture ANalysis Code 2D), which is based on the code FRANC2D [50,51] developed at Cornell University. The I-FRANC2D element library for FGMs consists of *graded elements* [19,46,45], which incorporate the material gradient at the size scale of the element. The specific graded elements used here are based on the *generalized isoparametric formulation* presented by Kim and Paulino [19], who have also compared the performance of these elements with that of conventional homogeneous elements which produce a step-wise constant approximation to a continuous material property field [45].

All the geometry is discretized with isoparametric graded elements [19]. The specific elements used consist of singular quarter-point six-node triangles (*T6qp*) for crack-tip discretization, eight-node serendipity elements (*Q8*) for a circular region around crack-tip elements, and regular six-node triangles (*T6*) in a transition zone to *Q*8 elements (see, for example, Fig. 6, for a typical crack tip region discretization).

All the examples consist of SIFs and *T* stress results for both isotropic and orthotropic FGMs, and those results are obtained by the interaction integral in conjunction with the FEM. In order to validate SIFs and *T* stress solutions, the FEM results for the first example (an inclined center crack in an exponentially graded plate

[4]The FEM code I-FRANC2D was formerly called FGM-FRANC2D [19].

Table 2 Example 1: comparison of normalized mixed-mode SIFs in *isotropic* FGMs for $\beta a = 0.5$ ($K_0 = \bar{\varepsilon} E^0 \sqrt{\pi a}$) (see Fig. 6). Contour 5 shown in Fig. 6(*c*) is used for the constant-constitutive-tensor formulation. The results for the nonequilibrium and incompatibility formulations are almost identical and thus the results from the latter formulation are not reported here.

Method	$\bar{\theta}$	K_I^+/K_0	K_{II}^+/K_0	K_I^-/K_0	K_{II}^-/K_0
Konda and Erdogan [47]	0°	1.424	0.000	0.674	0.000
	18°	1.285	0.344	0.617	0.213
	36°	0.925	0.548	0.460	0.365
	54°	0.490	0.532	0.247	0.397
	72°	0.146	0.314	0.059	0.269
	90°	0.000	0.000	0.000	0.000
Nonequilibrium	0°	1.4234	0.0000	0.6657	0.0000
	18°	1.2835	0.3454	0.6104	0.2112
	36°	0.9224	0.5502	0.4559	0.3625
	54°	0.4880	0.5338	0.2451	0.3943
	72°	0.1451	0.3147	0.0587	0.2670
	90°	0.0000	0.0000	0.0000	0.0000
Constant-constitutive tensor	0°	1.4262	0.0000	0.6629	0.0000
	18°	1.2807	0.3452	0.6081	0.2101
	36°	0.9224	0.5512	0.4546	0.3607
	54°	0.4862	0.5348	0.2460	0.3931
	72°	0.1439	0.3144	0.0596	0.2670
	90°	0.0000	0.0000	0.0000	0.0000
Dolbow and Gosz [8] (X-FEM)	0°	1.445	0.000	0.681	0.000
	18°	1.303	0.353	0.623	0.213
	36°	0.930	0.560	0.467	0.364
	54°	0.488	0.540	0.251	0.396
	72°	0.142	0.316	0.062	0.268
	90°	0.000	0.000	0.000	0.000

subjected to fixed-grip loading) are compared with available semi-analytical and numerical solutions. The second example involves hyperbolic-tangent functions for material properties and investigates the effect of translation of these properties with respect to the crack-tip location.

9.1 Inclined Center Crack in a Plate. Figure 6(*a*) shows an inclined center crack of length $2a$ located with a geometric angle $\bar{\theta}$ (counter-clockwise) in a plate subjected to fixed-grip loading; Fig. 6(*b*) shows the complete mesh configuration; Fig. 6(*c*) shows five contours used for EDI computation of the *M* integral; and Fig. 6(*d*) shows the mesh detail using 12 sectors (*S12*) and four rings (*R4*) of elements around the crack tips. The displacement boundary condition is prescribed such that $u_2 = 0$ along the lower edge, and $u_1 = 0$ for the node at the lower left-hand side. The mesh discretization consists of 1641 *Q8*, 94 *T6*, and 24 *T6qp* elements, with a total of 1759 elements and 5336 nodes. The fixed-grip loading results in a uniform strain $\varepsilon_{22}(X_1, X_2) = \bar{\varepsilon}$ in a corresponding uncracked structure, which corresponds to $\sigma_{22}(X_1, 10) = \bar{\varepsilon} \bar{E}^0 e^{\beta X_1}$ for isotropic FGMs and $\sigma_{22}(X_1, 10) = \bar{\varepsilon} \bar{E}_{22}^0 e^{\beta X_1}$ for orthotropic FGMs (see Fig. 6(*a*)). Young's moduli and shear modulus are exponential functions of X_1, while Poisson's ratio is constant. The following data were used in the FEM analyses:

plane stress, 2×2 Gauss quadrature

dimensionless nonhomogeneity parameter: $\beta a = 0.5$

$$a/W = 0.1, \quad L/W = 1.0, \quad \bar{\theta} = 0° \text{ to } 90°, \quad \bar{\varepsilon} = 1$$

Isotropic case

$$E(X_1) = E^0 e^{\beta X_1}, \quad \nu(X_1) = \nu$$

$$E^0 = 1.0, \quad \nu = 0.3$$

Orthotropic case

$$E_{11}(X_1) = E_{11}^0 e^{\beta X_1}, \quad E_{22}(X_1) = E_{22}^0 e^{\beta X_1},$$
$$G_{12}(X_1) = G_{12}^0 e^{\beta X_1}, \quad \nu_{12}(X_1) = \nu_{12}^0$$

$$E_{11}^0 = 10^4, \quad E_{22}^0 = 10^3, \quad G_{12}^0 = 1216, \quad \nu_{12}^0 = 0.3$$

Table 2 compares the present FEM results for normalized SIFs obtained by the nonequilibrium and constant-constitutive-tensor formulations of the *M* integral with semi-analytical solutions provided by Konda and Erdogan [47] and the extended FEM results by Dolbow and Gosz [8] for various geometric angles of a crack in isotropic FGMs. The difference in the result for SIFs between nonequilibrium and incompatibility formulations is found to be in the order $O(10^{-4})$ in this example, and thus the results are not provided. The converged results obtained by the nonequilibrium formulation are in good agreement with those by Konda and Erdogan [47] (maximum difference 1.3%, average difference 0.6%), those by Dolbow and Gosz [8], and those obtained by the constant-constitutive-tensor formulation. For the nonequilibrium and incompatibility formulations, a domain including almost half of the square plate is used, and converged solutions are obtained. However, for the constant-constitutive-tensor formulation, contour 5 as shown in Fig. 6(*c*) is used. We observe that the accuracy for the constant-constitutive-tensor formulation are reasonable for small size of contours such as contours 1–5, but as the contour becomes large than contour 5, the solution does not converge, and accuracy deteriorates. As explained in the theoretical discussion, the constant-constitutive-tensor formulation may have numerical problems in the accuracy of derivatives of actual strain or stress fields. To reduce domain dependence, mesh discretization over the plate shown in Fig. 6(*b*) needs to be improved.

Figure 7 shows $J = (K_I^2 + K_{II}^2)/E_{\text{tip}}$ value calculated by the interaction integral for the right crack tip of an inclined crack with $\bar{\theta} = 18$ deg using five contours for EDI computations as shown in Fig. 6(*c*). The nonequilibrium formulation is used both considering and neglecting the nonequilibrium term (see Eq. (22)), and the incompatibility formulation is used both considering and neglect-

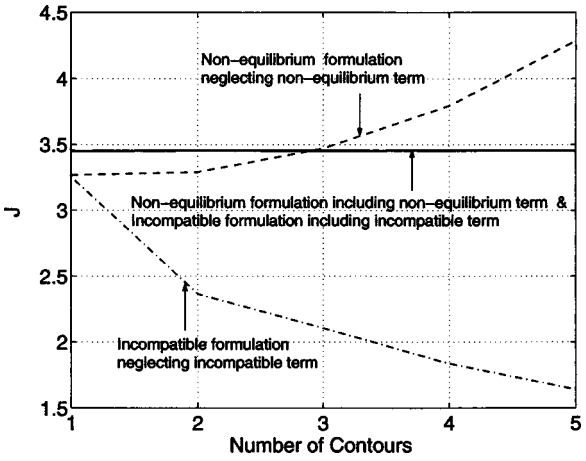

Fig. 7 Example 1: comparison of $J=(K_I^2+K_{II}^2)/E_{tip}$ for the right crack tip of an inclined crack with $\bar{\theta}=18°$ using the *M* integral. The nonequilibrium formulation is used both considering and neglecting the nonequilibrium term (see Eq. (22)). The incompatibility formulation is used both considering and neglecting the incompatible term (see Eq. (23))

ing the incompatible term (see Eq. (23)). The solutions obtained by considering the nonequilibrium term for the nonequilibrium formulation, and the incompatibility term for the incompatibility formulation are not distinguishable in a graphical form. Notice that the converged solution is obtained when including either the nonequilibrium or the incompatibility term, however, such behavior is generally not observed when neglecting either term.

Table 3 compares the present FEM results for normalized SIFs in orthotropic FGMs obtained by the nonequilibrium formulation of the *M* integral with those obtained by the incompatibility formulation for various geometric angles of a crack in orthotropic FGMs. Notice that the two formulations provide similar FEM results for SIFs for each geometric angle. Comparison of Tables 2 and 3 indicates that the material orthotropy shows significant effect on SIFs, and the SIFs K_I^+ (right crack tip) and K_{II}^- (left crack tip) for the orthotropic case are greater than or equal to those for the isotropic case, however, the SIFs K_{II}^+ and K_I^- for the orthotropic case are smaller than or equal to those that for the isotropic case.

Table 4 compares the present FEM results for normalized *T* stress in isotropic FGMs obtained by the nonequilibrium formulation of the *M*-integral with those reported by Paulino and Dong [48] who used the singular integral equation method. Table 5 compares the present FEM results for normalized *T* stress obtained by the nonequilibrium formulation of the *M* integral with those obtained by the incompatibility formulation for orthotropic FGMs. Notice that the two formulations provide similar FEM results for *T* stress for each geometric angle. For the isotropic case, *T* stress at both right and left crack tips changes sign in the range of angle $\bar{\theta}$=30 deg–45 deg (see Table 4), while, for the orthotropic case, it changes sign in the range of angle $\bar{\theta}$=15 deg–30 deg (see Table 5). Comparison of Tables 4 and 5 indicates that the material orthotropy shows significant effect on *T* stress in terms of both sign and magnitude.

Table 4 Example 1: comparison of normalized *T* stress in *isotropic* FGMs for $\beta a=0.5$ ($\sigma_0=\bar{\varepsilon}E^0$) (see Fig. 6)

	Nonequilibrium		Paulino and Dong [48]	
$\bar{\theta}$	$T(+a)/\sigma_0$	$T(-a)/\sigma_0$	$T(+a)/\sigma_0$	$T(-a)/\sigma_0$
0°	−0.896	−0.858	−0.867	−0.876
15°	−0.773	−0.747	−0.748	−0.763
30°	−0.434	−0.436	−0.420	−0.444
45°	0.036	0.011	0.039	0.010
60°	0.513	0.484	0.513	0.490
75°	0.868	0.850	0.870	0.858
90°	0.994	0.994	1.000	1.000

9.2 Strip With an Edge Crack. Figure 8(*a*) shows an edge crack of length "*a*" in a plate, and Fig. 8(*b*) shows the complete mesh discretization using 12 sectors (*S12*) and four rings (*R4*) of elements around the crack tip. Figures 8(*c*)–8(*e*) illustrate the three considered types of hyperbolic-tangent material gradation with respect to the crack tip: reference configuration, translation to the left, and translation to the right, respectively. The fixed-grip displacement loading results in a uniform strain $\varepsilon_{22}(X_1,X_2)=\bar{\varepsilon}$ in a corresponding uncracked structure. The displacement boundary condition is prescribed such that $u_2=0$ along the lower edge and $u_1=0$ for the node at the left-hand side. The mesh discretization consists of 208 *Q8*, 37 *T6*, and 12 *T6qp* elements, with a total of 257 elements and 1001 nodes.

Young's moduli and shear modulus are hyperbolic-tangent functions with respect to the global (X_1,X_2) Cartesian coordinates, while Poisson's ratio is constant (Fig. 9). The following data were used for the FEM analysis:

plane strain, 2×2 Gauss quadrature

$$a/W=0.5,\quad L/W=2.0,\quad \bar{\varepsilon}=0.25,\quad d=(-0.5 \text{ to } 0.5)$$

Isotropic case

$$E(X_1)=(E^-+E^+)/2+\tanh[\beta(X_1+d)](E^--E^+)/2$$

Table 3 Example 1: Comparison of normalized mixed-mode SIFs in *orthotropic* FGMs for $\beta a=0.5$ ($K_0=\bar{\varepsilon}E_{22}^0\sqrt{\pi a}$) (see Fig. 6)

Formulation	$\bar{\theta}$	K_I^+/K_0	K_{II}^+/K_0	K_I^-/K_0	K_{II}^-/K_0
Nonequilibrium	0°	1.4279	0.0000	0.6663	0.0000
	18°	1.3224	0.2176	0.5997	0.2436
	36°	1.0177	0.4097	0.4150	0.4160
	54°	0.6008	0.4477	0.1814	0.4379
	72°	0.2154	0.2906	0.0056	0.2822
	90°	0.0000	0.0000	0.0000	0.0000
Incompatiblity	0°	1.4285	0.0000	0.6663	0.0000
	18°	1.3224	0.2194	0.5997	0.2427
	36°	1.0177	0.4111	0.4149	0.4156
	54°	0.6008	0.4480	0.1809	0.4373
	72°	0.2158	0.2906	0.0052	0.2823
	90°	0.0000	0.0000	0.0000	0.0000

Table 5 Example 1: comparison of normalized *T* stress in *orthotropic* FGMs for $\beta a=0.5$ ($\sigma_0=\bar{\varepsilon}E^0_{22}$) (see Fig. 6)

	Nonequilibrium		Incompatibility	
$\bar{\theta}$	$T(+a)/\sigma_0$	$T(-a)/\sigma_0$	$T(+a)/\sigma_0$	$T(-a)/\sigma_0$
0°	−2.822	−2.725	−2.832	−2.712
15°	−1.407	−1.402	−1.384	−1.407
30°	0.156	0.079	0.168	0.074
45°	0.785	0.700	0.785	0.702
60°	0.971	0.909	0.970	0.910
75°	1.003	0.973	1.002	0.973
90°	0.996	0.996	0.997	0.997

$$\beta a = 15.0, \quad \nu = 0.3$$

$$(E^-, E^+) = (1.00, 3.00)$$

Orthotropic case

$$E_{11}(X_1) = (E^-_{11} + E^+_{11})/2 + \tanh[\alpha(X_1 + d)](E^-_{11} - E^+_{11})/2$$

$$E_{22}(X_1) = (E^-_{22} + E^+_{22})/2 + \tanh[\beta(X_1 + d)](E^-_{22} - E^+_{22})/2$$

$$G_{12}(X_1) = (G^-_{12} + G^+_{12})/2 + \tanh[\gamma(X_1 + d)](G^-_{12} - G^+_{12})/2$$

$$\alpha a = \beta a = \gamma a = 15.0, \quad \nu_{12} = 0.3$$

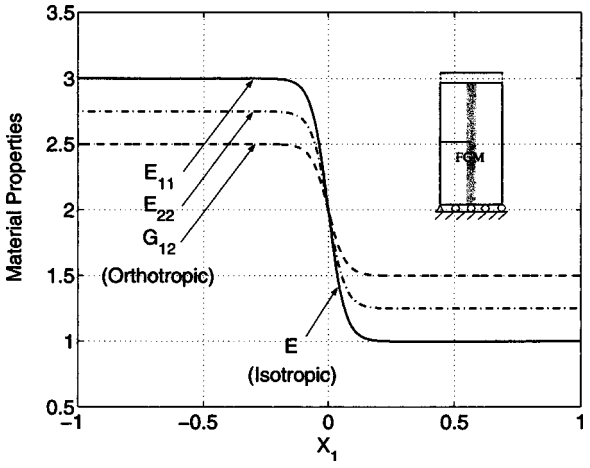

Fig. 9 Example 2: variation of material properties: E_{11}, E_{22}, and G_{12} for the orthotropic case, and E for the isotropic case

$$(E^-_{11}, E^+_{11}) = (1.00, 3.00), \quad (E^-_{22}, E^+_{22}) = (1.25, 2.75),$$
$$(G^-_{12}, G^+_{12}) = (1.50, 2.50)$$

Table 6 compares the present FEM results for mode I SIF (K_I) obtained by the nonequilibrium formulation with those obtained by the incompatibility formulation for various translation factors "*d*" of hyperbolic-tangent material variation considering both iso-

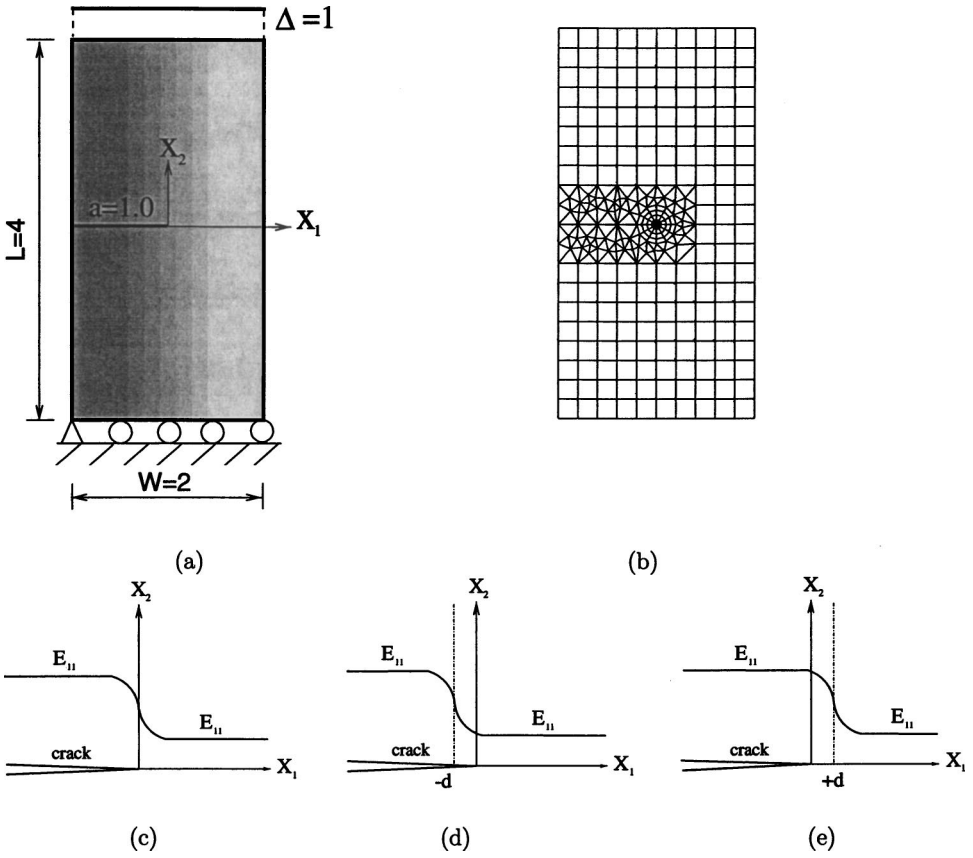

Fig. 8 Example 2: strip with an edge crack in hyperbolic-tangent materials: (*a*) geometry and BCs; (*b*) complete finite element mesh with 12 sectors (*S*12) and four rings (*R*4) around the crack tip; (*c*) reference configuration (*d*=0.0); (*d*) translation of material gradation to the left (*d*=+0.5); (*e*) translation of material gradation to the right (*d*=−0.5)

Table 6 Example 2: comparison of mode I SIF (K_I) for an edge crack considering translation (d) of hyperbolic-tangent material variation (see Fig. 8)

	Nonequilibrium		Incompatibility	
d	Iso	Ortho	Iso	Ortho [12]
−0.5	1.212	1.164	1.186	1.158
−0.4	1.211	1.167	1.201	1.163
−0.3	1.211	1.175	1.190	1.173
−0.2	1.218	1.189	1.209	1.189
−0.1	1.231	1.212	1.212	1.217
0	1.030	1.047	1.026	1.049
0.1	0.595	0.701	0.588	0.697
0.2	0.486	0.615	0.487	0.614
0.3	0.451	0.585	0.451	0.585
0.4	0.430	0.567	0.430	0.567
0.5	0.419	0.554	0.419	0.554

tropic and orthotropic FGMs. For the orthotropic case, the FEM results obtained by the nonequilibrium formulation are compared with those obtained by the incompatibility formulation reported by Kim and Paulino [12]. Notice that the two equivalent formulations provide similar FEM results for mode I SIF for each translation factor d. For the isotropic FGMs, the mode I SIF decreases with the translation factor d for the range between −0.1 and 0.5. For the orthotropic FGMs, the mode I SIF increases with the translation factor d for the range between −0.5 and −0.1, however, it decreases as d increases further. Table 6 also indicates that mode I SIFs for the orthotropic case are smaller than those for the isotropic case for each translation factor d from −0.5 to −0.1, however, the SIFs for the orthotropic case are greater than those for the isotropic case for $d=0$ to 0.5.

Table 7 compares the present FEM results for T stress obtained by the nonequilibrium formulation with those obtained by the incompatibility formulation for various translation factors d of hyperbolic-tangent material variation considering both isotropic and orthotropic FGMs. Notice that the two formulations provide similar FEM results, and the T stresses are negative for all the translation factors d considered. For both isotropic and orthotropic FGMs, the T stress decreases with the translation factor d for the range between −0.5 and 0.0, however, it increases as d increases further. Table 7 also indicates that T stress for the orthotropic case is greater than or equal to that for the isotropic case for each translation factor.

Table 7 Example 2: comparison of T stress for an edge crack considering translation (d) of hyperbolic-tangent material variation (see Fig. 8)

	Nonequilibrium		Incompatibility	
d	Iso	Ortho	Iso	Ortho
−0.5	−0.463	−0.393	−0.452	−0.394
−0.4	−0.478	−0.407	−0.470	−0.406
−0.3	−0.507	−0.434	−0.493	−0.439
−0.2	−0.580	−0.499	−0.571	−0.501
−0.1	−0.797	−0.686	−0.797	−0.702
0	−1.123	−0.923	−1.181	−0.962
0.1	−0.444	−0.364	−0.431	−0.362
0.2	−0.218	−0.205	−0.217	−0.205
0.3	−0.175	−0.171	−0.175	−0.171
0.4	−0.157	−0.157	−0.157	−0.157
0.5	−0.152	−0.151	−0.152	−0.152

10 Conclusions

This paper provides a critical assessment and comparison of three consistent formulations: nonequilibrium, incompatibility, and constant-constitutive-tensor formulations. Each formulation leads to a consistent form of the interaction integral in the sense that extra terms are added to compensate for the difference in response between homogeneous and nonhomogeneous materials. These extra terms play a key role in ensuring path independence of the interaction integral for FGMs. In terms of numerical computations, the nonequilibrium formulation leads to the simplest final form of the M integral among the three formulations. In terms of numerical accuracy, the nonequilibrium formulation is equivalent to the incompatibility formulation, which is observed in numerical examples involving various types of material gradation. The constant-constitutive-tensor formulation requires the derivatives of the actual stress and strain field, and may have numerical accuracy problems with standard C^0 elements commonly used in the displacement-based FEM, as observed in example 1.

From numerical investigations, we observe that both material gradation and orthotropy have a significant influence on SIFs and T stress (i.e., both sign and magnitude), and the crack tip location also shows a significant influence on the fracture parameters in hyperbolic-tangent materials. We also observe that the extra terms (e.g., nonequilibrium or incompatible terms) ensure convergence to target solutions (SIFs or T stress).

Acknowledgments

The authors gratefully acknowledge the support from NASA-Ames, Engineering for Complex Systems Program, and the NASA-Ames Chief Engineer (Dr. Tina Panontin) through Grant No. NAG 2-1424. They also acknowledge additional support from the National Science Foundation (NSF) under Grant No. CMS-0115954 (Mechanics and Materials Program).

Nomenclature

a = half crack length

$\boldsymbol{a}$ or a_{ij} = contracted notation of the compliance tensor ($\boldsymbol{S}$ or S_{ijkl}) for plane stress; $i=1,2,6$; $j=1,2,6$

$\boldsymbol{a}^{\text{tip}}$ or a_{ij}^{tip} = $\boldsymbol{a}$ or a_{ij} evaluated at the crack tip location; $i,j=1,2,6$

$\boldsymbol{A}$ = a 2×2 complex matrix

b_{ij} = contracted notation of the compliance tensor for plane strain; $i=1,2,6$; $j=1,2,6$

b_{ij}^{tip} = b_{ij} evaluated at the crack tip location; $i,j=1,2,6$

$\boldsymbol{B}$ = a 2×2 complex matrix

c_{11}, c_{22}, c_{12} = coefficients in the relationship between J and stress intensity factors (K_I and K_{II})

$\boldsymbol{C}(\boldsymbol{\theta})$ = a 2×2 diagonal matrix

C_{ijkl} or $\boldsymbol{C}$ = constitutive tensor; $i,j,k,l=1,2,3$

d = translation factor in hyperbolic-tangent function

d_0 = x_1 coordinate of a fixed point

e = natural logarithm base, $e=2.71828182\ldots$

E = Young's modulus for isotropic materials

E^0 = Young's modulus E evaluated at the origin

E_{tip} = Young's modulus E evaluated at the crack tip

E_{11}, E_{22} = Young's moduli with respect to the principal axes of orthotropy

E_{11}^0, E_{22}^0 = Young's moduli E_{11},E_{22} evaluated at the origin

f = a point force

$\boldsymbol{f}$ = a 2×1 force vector

$\boldsymbol{f}^I$, $\boldsymbol{f}^{II}$ = representative functions for auxiliary displacements for SIFs

G_{12} = shear modulus for orthotropic materials

G_{12}^0 = shear modulus G_{12} evaluated at the origin
$\mathcal{G}$ = energe release rates
$\boldsymbol{g}^I$, $\boldsymbol{g}^{II}$ = representative functions for auxiliary stresses for SIFs
$\mathcal{G}_I$ = mode I energe release rate
$\mathcal{G}_{II}$ = mode II energe release rate
$\mathcal{H}$ = contour integral
$\boldsymbol{h}$ = a 2×1 real matrix
Im = imaginary part of the complex function
J = path-independent J integral for the actual field
J^{aux} = J integral for the auxiliary field
J^s = J integral for the superimposed fields (actual plus auxiliary)
K_I = mode I stress intensity factor
K_{II} = mode II stress intensity factor
K_0 = normalizing factor for stress intensity factors, $K_0=\overline{\varepsilon}\overline{E}^0\sqrt{\pi a}$ for the isotropic case and $K_0=\overline{\varepsilon}\overline{E}_{22}^0\sqrt{\pi a}$ for the orthotropic case
L = length of a plate
$\boldsymbol{L}$ = a 2×2 real matrix
M = interaction integral (M integral)
N_i = shape functions for node i of an element
$\boldsymbol{N}_3(\boldsymbol{\theta})$ = a 2×2 real matrix
m_i, n_i = unit normal vectors on the contour of the domain integral
P = a generic property (C_{ijkl}, S_{ijkl}, or ε_{ij})
$\boldsymbol{P}(\boldsymbol{\theta})$ = a 2×2 diagonal matrix
p_k = coefficients of the asymptotic displacements for orthotropic materials; $k=1,2$
q_k = coefficients of the asymptotic displacements for orthotropic materials; $k=1,2$
q = weight function in the domain integral
r = radial direction in polar coordinates
Re = real part of the complex function
S_{ijkl} or $\boldsymbol{S}$ = compliance tensor; $i,j,k,l=1,2,3$
$\boldsymbol{S}(\boldsymbol{\theta})$ = a 2×2 real matrix
T = elastic T stress
$\boldsymbol{t}^u$ = representative functions for auxiliary displacements for T stress
$\boldsymbol{t}^s$ = representative functions for auxiliary stresses for T stress
u_i = displacements for the actual field; $i=1,2$
$\boldsymbol{u}^{\text{aux}}$ or u_i^{aux} = a vector for auxiliary displacements; $i=1,2$
W = width of a plate
$\mathcal{W}$ = strain energy density
$\mathcal{W}^{\text{aux}}$ = strain energy density for the auxiliary field
x_i = local Cartesian coordinates; $i=1,2$
X_i = global Cartesian coordinates; $i=1,2$
z_k = complex variable, $z_k=x_k+iy_k$; $k=1,2$
α = material nonhomogeneity parameter for gradation of E_{11}
α_k = the real part of μ_k; $k=1,2$
β = material nonhomogeneity parameter for gradation of E_{22} or E
β_k = the imaginary part of μ_k; $k=1,2$
γ = material nonhomogeneity parameter for gradation of G_{12}
Γ = contour for J and M integrals
Γ_0 = outer contour
Γ_s = inner contour
Γ^+ = contour along the upper crack face
Γ^- = contour along the lower crack face
δ_{ij} = Kronecker delta; $i,j=1,2$
ε_{ij} = strains for the actual field; $i=1,2,3$; $j=1,2,3$
ε_k = contracted notation of ε_{ij}; $k=1,\ldots,6$
$\boldsymbol{\varepsilon}^{\text{aux}}$ or $\varepsilon_{ij}^{\text{aux}}$ = a vector for auxiliary strains; $i,j=1,2,3$
θ = angular direction in polar coordinates with respect to the local Cartesian coordinates
$\overline{\theta}$ = the angle of the local Cartesian coordinates with respect to the global Cartesian coordinates
θ_m = indication of direction of material gradation with respect to the crack
κ = material parameter for isotropic materials; $(3-\nu)/(1+\nu)$ for plane stress and $3-4\nu$ for plane strain
κ^{tip} = material parameter κ evaluated at the crack tip
μ_k = roots of the characteristic equation; $k=1,2$
μ_k^{tip} = μ_k evaluated at the crack tip location; $k=1,2$
$\overline{\mu_k}$ = complex conjugate of μ_k; $k=1,2$
ν = Poisson's ratio for isotropic materials
ν_{12}, ν_{21} = Poisson's ratios for orthotropic materials
σ_k = contracted notation of σ_{ij}; $k=1,\ldots,6$
σ_0 = normalizing factor; $\sigma_0=\overline{\varepsilon}\overline{E}^0$ for the isotropic case $\sigma_0=\overline{\varepsilon}\overline{E}_{22}^0$ for the orthotropic case
σ_{ij} = stresses for the actual fields; $i=1,2,3$; $j=1,2,3$
$\boldsymbol{\sigma}^{\text{aux}}$ or σ_{ij}^{aux} = a vector for auxiliary stresses; $i,j=1,2,3$

Appendix A: Anisotropic Elasticity

The generalized Hooke's law for stress-strain relationship is given by [40]:

$$\varepsilon_i = a_{ij}\sigma_j, \quad a_{ij} = a_{ji}(i,j=1,2,\ldots,6) \tag{A1}$$

where the compliance coefficients, a_{ij}, are contracted notations of the compliance tensor S_{ijkl} and

$$\varepsilon_1=\varepsilon_{11}, \quad \varepsilon_2=\varepsilon_{22}, \quad \varepsilon_3=\varepsilon_{33}, \quad \varepsilon_4=2\varepsilon_{23}, \quad \varepsilon_5=2\varepsilon_{13},$$
$$\varepsilon_6=2\varepsilon_{12}$$

$$\sigma_1=\sigma_{11}, \quad \sigma_2=\sigma_{22}, \quad \sigma_3=\sigma_{33}, \quad \sigma_4=\sigma_{23}, \quad \sigma_5=\sigma_{13}, \quad \sigma_6=\sigma_{12} \tag{A2}$$

For plane stress, the a_{ij} components of interest are

$$a_{ij}(i,j=1,2,6) \tag{A3}$$

and for plane strain, the a_{ij} components are exchanged with b_{ij} as follows:

$$b_{ij} = a_{ij} - \frac{a_{i3}a_{j3}}{a_{33}}(i,j=1,2,6) \tag{A4}$$

Two-dimensional anisotropic elasticity problems can be formulated in terms of the analytic functions, $\phi_k(z_k)$, of the complex variable, $z_k=x_k+iy_k$ $(k=1,2)$, $i=\sqrt{-1}$, where

$$x_k = x+\alpha_k y, \quad y_k=\beta_k y(k=1,2) \tag{A5}$$

The parameters α_k and β_k are the real and imaginary parts of $\mu_k=\alpha_k+i\beta_k$, which can be determined from the following characteristic equation [40]:

$$a_{11}\mu^4 - 2a_{16}\mu^3 + (2a_{12}+a_{66})\mu^2 - 2a_{26}\mu + a_{22} = 0 \tag{A6}$$

where the roots μ_k are always complex or purely imaginary in conjugate pairs as $\mu_1,\overline{\mu_1};\mu_2,\overline{\mu_2}$.

Appendix B: Representative Functions for SIFs

For orthotropic FGMs, the representative functions $\boldsymbol{f}(r^{1/2},\theta,\boldsymbol{a}^{\text{tip}})$ in Eq. (1) are given by [37]:

$$f_1^I = \sqrt{2r/\pi}\,\mathrm{Re}\left[\frac{1}{\mu_1^{\mathrm{tip}}-\mu_2^{\mathrm{tip}}}\{\mu_1^{\mathrm{tip}}p_2\sqrt{\cos\theta+\mu_2^{\mathrm{tip}}\sin\theta} - \mu_2^{\mathrm{tip}}p_1\sqrt{\cos\theta+\mu_1^{\mathrm{tip}}\sin\theta}\}\right]$$

$$f_1^{II} = \sqrt{2r/\pi}\,\mathrm{Re}\left[\frac{1}{\mu_1^{\mathrm{tip}}-\mu_2^{\mathrm{tip}}}\{p_2\sqrt{\cos\theta+\mu_2^{\mathrm{tip}}\sin\theta} - p_1\sqrt{\cos\theta+\mu_1^{\mathrm{tip}}\sin\theta}\}\right]$$

$$f_2^I = \sqrt{2r/\pi}\,\mathrm{Re}\left[\frac{1}{\mu_1^{\mathrm{tip}}-\mu_2^{\mathrm{tip}}}\{\mu_1^{\mathrm{tip}}q_2\sqrt{\cos\theta+\mu_2^{\mathrm{tip}}\sin\theta} - \mu_2^{\mathrm{tip}}q_1\sqrt{\cos\theta+\mu_1^{\mathrm{tip}}\sin\theta}\}\right]$$

$$f_2^{II} = \sqrt{2r/\pi}\,\mathrm{Re}\left[\frac{1}{\mu_1^{\mathrm{tip}}-\mu_2^{\mathrm{tip}}}\{q_2\sqrt{\cos\theta+\mu_2^{\mathrm{tip}}\sin\theta} - q_1\sqrt{\cos\theta+\mu_1^{\mathrm{tip}}\sin\theta}\}\right]$$

where Re denotes the real part of the complex function, μ_1^{tip} and μ_2^{tip} denote crack-tip material parameters, which are obtained from Eq. (A6) and taken for $\beta_k > 0$ ($k=1,2$), and p_k and q_k are given by

$$p_k = a_{11}^{\mathrm{tip}}(\mu_k^{\mathrm{tip}})^2 + a_{12}^{\mathrm{tip}} - a_{16}^{\mathrm{tip}}\mu_k^{\mathrm{tip}}$$

$$q_k = a_{12}^{\mathrm{tip}}\mu_k^{\mathrm{tip}} + \frac{a_{22}^{\mathrm{tip}}}{\mu_k^{\mathrm{tip}}} - a_{26}^{\mathrm{tip}} \tag{B1}$$

respectively. The functions $\boldsymbol{g}(r^{-1/2},\theta,\boldsymbol{a}^{\mathrm{tip}})$ in Eq. (3) are given by [37]:

$$g_{11}^I = \frac{1}{\sqrt{2\pi r}}\,\mathrm{Re}\left[\frac{\mu_1^{\mathrm{tip}}\mu_2^{\mathrm{tip}}}{\mu_1^{\mathrm{tip}}-\mu_2^{\mathrm{tip}}}\left\{\frac{\mu_2^{\mathrm{tip}}}{\sqrt{\cos\theta+\mu_2^{\mathrm{tip}}\sin\theta}} - \frac{\mu_1^{\mathrm{tip}}}{\sqrt{\cos\theta+\mu_1^{\mathrm{tip}}\sin\theta}}\right\}\right]$$

$$g_{11}^{II} = \frac{1}{\sqrt{2\pi r}}\,\mathrm{Re}\left[\frac{1}{\mu_1^{\mathrm{tip}}-\mu_2^{\mathrm{tip}}}\left\{\frac{(\mu_2^{\mathrm{tip}})^2}{\sqrt{\cos\theta+\mu_2^{\mathrm{tip}}\sin\theta}} - \frac{(\mu_1^{\mathrm{tip}})^2}{\sqrt{\cos\theta+\mu_1^{\mathrm{tip}}\sin\theta}}\right\}\right]$$

$$g_{22}^I = \frac{1}{\sqrt{2\pi r}}\,\mathrm{Re}\left[\frac{1}{\mu_1^{\mathrm{tip}}-\mu_2^{\mathrm{tip}}}\left\{\frac{\mu_1^{\mathrm{tip}}}{\sqrt{\cos\theta+\mu_2^{\mathrm{tip}}\sin\theta}} - \frac{\mu_2^{\mathrm{tip}}}{\sqrt{\cos\theta+\mu_1^{\mathrm{tip}}\sin\theta}}\right\}\right]$$

$$g_{22}^{II} = \frac{1}{\sqrt{2\pi r}}\,\mathrm{Re}\left[\frac{1}{\mu_1^{\mathrm{tip}}-\mu_2^{\mathrm{tip}}}\left\{\frac{1}{\sqrt{\cos\theta+\mu_2^{\mathrm{tip}}\sin\theta}} - \frac{1}{\sqrt{\cos\theta+\mu_1^{\mathrm{tip}}\sin\theta}}\right\}\right]$$

$$g_{12}^I = \frac{1}{\sqrt{2\pi r}}\,\mathrm{Re}\left[\frac{\mu_1^{\mathrm{tip}}\mu_2^{\mathrm{tip}}}{\mu_1^{\mathrm{tip}}-\mu_2^{\mathrm{tip}}}\left\{\frac{1}{\sqrt{\cos\theta+\mu_1^{\mathrm{tip}}\sin\theta}} - \frac{1}{\sqrt{\cos\theta+\mu_2^{\mathrm{tip}}\sin\theta}}\right\}\right]$$

$$g_{12}^{II} = \frac{1}{\sqrt{2\pi r}}\,\mathrm{Re}\left[\frac{1}{\mu_1^{\mathrm{tip}}-\mu_2^{\mathrm{tip}}}\left\{\frac{\mu_1^{\mathrm{tip}}}{\sqrt{\cos\theta+\mu_1^{\mathrm{tip}}\sin\theta}} - \frac{\mu_2^{\mathrm{tip}}}{\sqrt{\cos\theta+\mu_2^{\mathrm{tip}}\sin\theta}}\right\}\right] \tag{B2}$$

Notice that, in the earlier expressions, the graded material parameters are sampled at the crack tip.

For isotropic FGMs, the representative functions $\boldsymbol{f}(r^{1/2},\theta,\boldsymbol{a}^{\mathrm{tip}})$ for displacements in Eq. (1), and $\boldsymbol{g}(r^{-1/2},\theta,\boldsymbol{a}^{\mathrm{tip}})$ for stresses in Eq. (3) are given in many references (e.g., Ref. [38]). The graded material parameters are sampled at the crack tip.

Appendix C: Representative Functions for *T* Stress

The presentation follows the Stroh formalism [39]. For othotropic FGMs, the representative functions $\boldsymbol{t}^u(\ln r,\theta,f,\boldsymbol{a}^{\mathrm{tip}})$ in Eq. (4) are given by [39]:

$$t_1^u = -\frac{h_1}{2\pi}\ln r - \frac{1}{2}(S_{11}h_1 + S_{12}h_2)$$

$$t_2^u = -\frac{h_2}{2\pi}\ln r - \frac{1}{2}(S_{21}h_1 + S_{22}h_2) \tag{C1}$$

The parameters S_{ij} and h_i in Eq. (C1) are the components in the 2×2 matrix $\boldsymbol{S}(\theta)$, and the 2×1 vector $\boldsymbol{h}$ as follows:

$$\boldsymbol{S}(\theta) = \frac{2}{\pi}\,\mathrm{Re}[\boldsymbol{A}\boldsymbol{C}(\theta)\boldsymbol{B}^T] = \begin{bmatrix} S_{11} & S_{12} \\ S_{21} & S_{22}\end{bmatrix}$$

$$\boldsymbol{h} = \boldsymbol{L}^{-1}\boldsymbol{f} = \begin{Bmatrix} h_1 \\ h_2\end{Bmatrix} \tag{C2}$$

where

$$\boldsymbol{A} = \begin{bmatrix} \lambda_1^{\mathrm{tip}}p_1^{\mathrm{tip}} & \lambda_2^{\mathrm{tip}}p_2^{\mathrm{tip}} \\ \lambda_1^{\mathrm{tip}}q_1^{\mathrm{tip}} & \lambda_2^{\mathrm{tip}}q_2^{\mathrm{tip}}\end{bmatrix},\quad \boldsymbol{B} = \begin{bmatrix} -\lambda_1^{\mathrm{tip}}\mu_1^{\mathrm{tip}} & -\lambda_2^{\mathrm{tip}}\mu_2^{\mathrm{tip}} \\ \lambda_1^{\mathrm{tip}} & \lambda_2^{\mathrm{tip}}\end{bmatrix}$$

$$\boldsymbol{C}(\theta) = \begin{bmatrix} \ln s_1(\theta) & 0 \\ 0 & \ln s_2(\theta)\end{bmatrix},\quad s_k(\theta) = \cos\theta + \mu_2^{\mathrm{tip}}\sin\theta$$

$$\boldsymbol{L}^{-1} = \mathrm{Re}[i\boldsymbol{A}\boldsymbol{B}^{-1}],\quad \boldsymbol{f} = [f,0]^T \tag{C3}$$

in which p_k^{tip} and q_k^{tip} ($k=1,2$) are given by Eq. (B1), and λ_k^{tip} ($k=1,2$) is the normalization factor given by the expression

$$2(\lambda_k^{\mathrm{tip}})^2(q_k^{\mathrm{tip}}/\mu_k^{\mathrm{tip}} - \mu_k^{\mathrm{tip}}p_k^{\mathrm{tip}}) = 1. \tag{C4}$$

The representative functions $\boldsymbol{t}^s(r^{-1},\theta,f,\boldsymbol{a}^{\mathrm{tip}})$ in Eq. (6) are given by [39]:

$$t_{11}^s = \sigma_{rr}^{\mathrm{aux}}\cos^2\theta,\quad t_{22}^s = \sigma_{rr}^{\mathrm{aux}}\sin^2\theta,\quad t_{12}^s = \sigma_{rr}^{\mathrm{aux}}\sin\theta\cos\theta \tag{C5}$$

where the auxiliary stresses are given by [39]:

$$\sigma_{rr}^{\mathrm{aux}} = \frac{1}{2\pi r}\boldsymbol{n}^T(\theta)\boldsymbol{N}_3(\theta)\boldsymbol{h},\quad \sigma_{\theta\theta}^{\mathrm{aux}} = \sigma_{r\theta}^{\mathrm{aux}} = 0 \tag{C6}$$

in which

$$\boldsymbol{n} = [\cos\theta,\sin\theta]^T,\quad \boldsymbol{N}_3(\theta) = 2\,\mathrm{Re}[\boldsymbol{B}\boldsymbol{P}(\theta)\boldsymbol{B}^T]$$

$$\boldsymbol{P}(\theta) = \begin{bmatrix} \mu_1(\theta) & 0 \\ 0 & \mu_2(\theta)\end{bmatrix},\quad \mu_k(\theta) = \frac{\mu_k^{\mathrm{tip}}\cos\theta - \sin\theta}{\mu_k^{\mathrm{tip}}\sin\theta + \cos\theta},\quad (k=1,2) \tag{C7}$$

For isotropic FGMs, the representative functions $\boldsymbol{t}^u(\ln r,\theta,f,\boldsymbol{a}^{\mathrm{tip}})$ in Eq. (4) for displacements, and $\boldsymbol{t}^s(r^{-1},\theta,f,\boldsymbol{a}^{\mathrm{tip}})$ for stresses in Eq. (6) are given in many references (e.g., Ref. [41]). The graded material parameters are sampled at the crack tip.

References

[1] Knowles, J. K., and Sternberg, E., 1972, "On a Class of Conservation Laws in Linearized and Finite Elastostatics," Arch. Ration. Mech. Anal., **44**(2), pp. 187–211.

[2] Budiansky, B., and Rice, J. R., 1973, "Conservation Laws and Energy-Release Rates," ASME J. Appl. Mech., **40**(1), pp. 201–203.

[3] Chang, J. H., and Chien, A. J., 2002, "Evaluation of M-Integral for Anisotropic Elastic Media With Multiple Defects," Int. J. Fract., **114**(3), pp. 267–289.

[4] Kanninen, M. F., and Popelar, C. H., 1985, *Advanced Fracture Mechanics*, Oxford University Press, New York.

[5] Yau, J. F., Wang, S. S., and Corten, H. T., 1980, "A Mixed-Mode Crack Analysis of Isotropic Solids Using Conservation Laws of Elasticity," ASME J. Appl. Mech., **47**(2), pp. 335–341.

[6] Wang, S. S., Corten, H. T., and Yau, J. F., 1980, "Mixed-Mode Crack Analysis of Rectilinear Anisotropic Solids Using Conservation Laws of Elasticity," Int. J. Fract., **16**(3), pp. 247–259.

[7] Yau, J. F., 1979, "Mixed-Mode Fracture Analysis Using a Conservation Integral," PhD thesis, Department of Theoretical and Applied Mechanics, University of Illinois at Urbana-Champaign.

[8] Dolbow, J., and Gosz, M., 2002, "On the Computation of Mixed-Mode Stress Intensity Factors in Functionally Graded Materials," Int. J. Solids Struct., **39**(9), pp. 2557–2574.

[9] Rao, B. N., and Rahman, S., 2003, "Mesh-Free Analysis of Cracks in Isotropic Functionally Graded Materials," Eng. Fract. Mech., **70**(1), pp. 1–27.

[10] Kim, J.-H., and Paulino, G. H., 2003, "An Accurate Scheme for Mixed-Mode Fracture Analysis of Functionally Graded Materials Using the Interaction Integral and Micromechanics Models," Int. J. Numer. Methods Eng., **58**(10), pp. 1457–1497.

[11] Kim, J.-H., and Paulino, G. H., 2003, "T-Stress, Mixed-Mode Stress Intensity Factors, and Crack Initiation Angles in Functionally Graded Materials: A Unified Approach Using the Interaction Integral Method," Comput. Methods Appl. Mech. Eng., **192**(11–12), pp. 1463–1494.

[12] Kim, J.-H., and Paulino, G. H., 2004, "T-Stress in Orthotropic Functionally Graded Materials: Lekhnitskii and Stroh Formalisms," Int. J. Fract., **126**(4), pp. 345–389.

[13] Eischen, J. W., 1987, "Fracture of Non-Homogeneous Materials," Int. J. Fract., **34**(1), pp. 3–22.

[14] Gu, P., Dao, M., and Asaro, R. J., 1997, "A Simplified Method for Calculating the Crack-Tip Field of Functionally Graded Materials Using the Domain Integral," ASME J. Appl. Mech., **34**(1), pp. 1–17.

[15] Anlas, G., Santare, M. H., and Lambros, J., 2000, "Numerical Calculation of Stress Intensity Factors in Functionally Graded Materials," Int. J. Fract., **104**(2), pp. 131–143.

[16] Marur, P. R., and Tippur, H. V., 2000, "Numerical Analysis of Crack-Tip Fields in Functionally Graded Materials With a Crack Normal to the Elastic Gradient," Int. J. Solids Struct., **37**(38), pp. 5353–5370.

[17] Bao, G., and Cai, H., 1997, "Delamination Cracking in Functionally Graded Coating/Metal Substrate Systems," Acta Mech., **45**(3), pp. 1055–1066.

[18] Bao, G., and Wang, L., 1995, "Multiple Cracking in Functionally Graded Ceramic/Metal Coatings," Int. J. Solids Struct., **32**(19), pp. 2853–2871.

[19] Kim, J.-H., and Paulino, G. H., 2002, "Finite Element Evaluation of Mixed-Mode Stress Intensity Factors in Functionally Graded Materials," Int. J. Numer. Methods Eng., **53**(8), pp. 1903–1935.

[20] Kim, J.-H., and Paulino, G. H., 2002, "Mixed-Mode Fracture of Orthotropic Functionally Graded Materials Using Finite Elements and the Modified Crack Closure Method," Eng. Fract. Mech., **69**(14–16), pp. 1557–1586.

[21] Kim, J.-H., and Paulino, G. H., 2003, "Mixed-Mode J-Integral Formulation and Implementation Using Graded Finite Elements for Fracture Analysis of Nonhomogeneous Orthotropic Materials," Mech. Mater., **35**(1–2), pp. 107–128.

[22] Williams, M. L., 1957, "On the Stress Distribution at the Base of a Stationary Crack," ASME J. Appl. Mech., **24**(1), pp. 109–114.

[23] Becker, T. L., Jr., Cannon, R. M., and Ritchie, R. O., 2001, "Finite Crack Kinking and T-Stresses in Functionally Graded Materials," Int. J. Solids Struct., **38**(32–33), pp. 5545–5563.

[24] Erdogan, F., 1995, "Fracture Mechanics of Functionally Graded Materials," Composites Eng., **5**(7), pp. 753–770.

[25] Noda, N., 1999, "Thermal Stresses in Functionally Graded Materials," J. Therm. Stresses, **22**(4–5), pp. 477–512.

[26] Paulino, G. H., Jin, Z. H., and Dodds, R. H., Jr., 2003, "Failure of Functionally Graded Materials." *Comprehensive Structural Integrity*, B. Karihaloo and W. G. Knauss, eds., Elsevier Science, New York, Vol. 2, Chap. 13, pp. 607–644.

[27] Delale, F., and Erdogan, F., 1983, "The Crack Problem for a Nonhomogeneous Plane," ASME J. Appl. Mech., **50**(3), pp. 609–614.

[28] Erdogan, F, and Wu, B. H., 1997, "The Surface Crack Problem for a Plate With Functionally Graded Properties," ASME J. Appl. Mech., **64**(3), pp. 449–456.

[29] Chan, Y.-S., Paulino, G. H., and Fannjiang, A. C., 2001, "The Crack Problem for Nonhomogeneous Materials Under Antiplane Shear Loading—A Displacement Based Formulation," Int. J. Solids Struct., **38**(17), pp. 2989–3005.

[30] Delale, F., and Erdogan, F., 1988, "On the Mechanical Modeling of an Interfacial Region in Bonded Half-Planes," ASME J. Appl. Mech., **55**(2), pp. 317–324.

[31] Gu, P., and Asaro, R. J., 1997, "Cracks in Functionally Graded Materials," Int. J. Solids Struct., **34**(1), pp. 1–17.

[32] Shbeeb, N. I., Binienda, W. K., and Kreider, K. L., 1999, "Analysis of the Driving Forces for Multiple Cracks in an Infinite Nonhomogeneous Plate, Part I: Theoretical Analysis," ASME J. Appl. Mech., **66**(2), pp. 492–500.

[33] Shbeeb, N. I., Binienda, W. K., and Kreider, K. L., 1999, "Analysis of the Driving Forces for Multiple Cracks in an Infinite Nonhomogeneous Plate, Part II: Numerical Solutions," ASME J. Appl. Mech., **66**(2), pp. 501–506.

[34] Honein, T., and Herrmann, G., 1997, "Conservation Laws in Nonhomogeneous Plane Elastostatics," J. Mech. Phys. Solids, **45**(5), pp. 789–805.

[35] Ozturk, M., and Erdogan, F., 1997, "Mode I Crack Problem in an Inhomogeneous Orthotropic Medium," Int. J. Eng. Sci., **35**(9), pp. 869–883.

[36] Ozturk, M., and Erdogan, F., 1999, "The Mixed Mode Crack Problem in an Inhomogeneous Orthotropic Medium," Int. J. Fract., **98**(3–4), pp. 243–261.

[37] Sih, G. C., Paris, P. C., and Irwin, G. R., 1965, "On Cracks in Rectilinearly Anisotropic Bodies," Int. J. Fract. Mech., **1**(2), pp. 189–203.

[38] Eftis, J., Subramonian, N., and Liebowitz, H., 1977, "Crack Border Atress and Displacement Equations Revisited," Eng. Fract. Mech., **9**(1), pp. 189–210.

[39] Ting, C. T. C., 1996, *Anisotropic Elasticity: Theory and Applications*, Oxford University Press, Oxford.

[40] Lekhnitskii, S. G., 1968, *Anisotropic Plates*, Gordon and Breach Science, New York.

[41] Michell, J. H., 1900, "Elementary Distributions of Plane Stress," Proc. London Math. Soc., **32**, pp. 35–61.

[42] Rice, J. R., 1968, "A Path-Independent Integral and the Approximate Analysis of Strain Concentration By Notches and Cracks," ASME J. Appl. Mech., **35**(2), pp. 379–386.

[43] Kim, J.-H., 2003, "Mixed-Mode Crack Propagation in Functionally Graded Materials," PhD thesis, University of Illinois at Urbana-Champaign.

[44] Paulino, G. H., and Kim, J.-H., 2004, "A New Approach to Compute T-Stress in Functionally Graded Materials Using the Interaction Integral Method," Eng. Fract. Mech., **71**(13–14), pp. 1907–1950.

[45] Kim, J.-H., and Paulino, G. H., 2002, "Isoparametric Graded Finite Elements for Nonhomogeneous Isotropic and Orthotropic Materials," ASME J. Appl. Mech., **69**(4), pp. 502–514.

[46] Santare, M. H., and Lambros, J., 2000, "Use of Graded Finite Elements to Model the Behavior of Nonhomogeneous Materials," ASME J. Appl. Mech., **67**(4), pp. 819–822.

[47] Konda, N., and Erdogan, F., 1994, "The Mixed Mode Crack Problem in a Nonhomogeneous Elastic Medium," Eng. Fract. Mech., **47**(4), pp. 533–545.

[48] Paulino, G. H., and Dong, Z. (unpublished).

[49] Cook, R. D., Malkus, D. S., Plesha, M. E., and Witt, R. J., 2001, *Concepts and Applications of Finite Element Analysis*, 4th ed., Wiley, New York.

[50] Wawrzynek, P. A., 1987, "Interactive Finite Element Analysis of Fracture Processes: An Integrated Approach," MS thesis, Cornell University.

[51] Wawrzynek, P. A., and Ingraffea, A. R., 1991, "Discrete Modeling of Crack Propagation: Theoretical Aspects and Implementation Issues in Two and Three Dimensions," Report 91-5, School of Civil Engineering and Environmental Engineering, Cornell University.